TEMPORAL VARIATION OF ELEMENTAL STOICHIOMETRY IN FRESHWATER PLANKTON

by

HAILEE MERSINO

A thesis submitted in partial fulfillment of the
requirements for the degree of

MASTERS OF SCIENCE IN BIOLOGY

2025

Oakland University
Rochester, Michigan

Thesis Advisory Committee:

Nicole Wagner, Ph.D., Chair
Clay Prater, Ph.D.
Tom Raffel, Ph.D.

© by Hailee Mersino, 2025
All rights reserved

This work is dedicated to myself, my partner, and my family.

ACKNOWLEDGMENTS

The completion of this work would not have been possible without the expertise and guidance of my supervisor, Dr. Nicole Wagner. Her standards have continuously pushed me to elevate both my work and myself. I would also like to thank my committee members, Dr. Clay Prater and Dr. Tom Raffel, for their input and flexibility throughout this process.

I am deeply grateful to Deryl Bernard and Carrie Spender from Seven Ponds Nature Center for granting access to their lakes and for their willingness in supporting our research. I am also appreciative of the opportunity to complete this degree with funding provided by Oakland University, where I have been fortunate to complete my bachelor's and now, master's degree.

I would like to thank those that have been directly involved in this project; my fellow lab members, Olivia Sowa and Ryan Andrews, for their collaboration, encouragement, and friendship; as well as our dedicated undergraduate students, Lillian Lesperance-Solomonson, Kaila Rahbornoohi, and Ava Hansen, for their shared enthusiasm, curiosity, and commitment to science and learning.

Most of all, I would like to thank my friends, family, and my partner, Alec, for their endless support, and for never admitting that they were sick of looking at my zooplankton pictures.

Hailee Mersino

ABSTRACT

TEMPORAL VARIATION OF ELEMENTAL STOICHIOMETRY IN FRESHWATER PLANKTON

by

Hailee Mersino

Advisor: Nicole Wagner, Ph.D.

The balance of elements within aquatic food webs shapes ecosystem productivity, energy transfer, and nutrient cycling, yet how this balance varies across space and time in freshwater systems remain poorly understood. Much of stoichiometric research in freshwater communities has focused on how macronutrients such as carbon (C), nitrogen (N), and phosphorus (P) move through food webs. Far less is known about how environmental drivers shape consumer stoichiometry, and the entire elemental profile of freshwater communities (i.e. the ionome). To address this, we examined temporal dynamics of seston and zooplankton in Tree Top Pond, a small, dimictic, eutrophic lake located within Seven Ponds Nature Center (Dryden, MI, USA), from March to September 2024. Temperature profiles were obtained from loggers deployed from the surface to the bottom of the lake to capture thermal variation through time. Zooplankton were sampled weekly to quantify the elemental composition (%C, %N, and %P) of two taxa, *Daphnia* and copepods, alongside community composition through time. Seston was sampled weekly at 1m intervals throughout the water column to characterize the ionomic profile.

We found that seston composition had inconsistent influence on zooplankton stoichiometry, while temperature had a stronger effect on elemental composition, particularly in *Daphnia*. Notably, %P in *Daphnia* and copepods converged over the season, suggesting that warming may alter biochemical allocation of nutrients. Seston ionomic dynamics, in contrast, were more strongly structured by spatiotemporal patterns and physical processes. Spring mixing characterized the seston ionome through geochemical influences of sediment-associated elements, such as aluminum (Al), manganese (Mn), and iron (Fe); whereas macronutrients, such as C, N, and P, were more influential. Across these dynamics, temperature significantly correlated with the concentration of many elements. These results demonstrate that consumer stoichiometry is differentially sensitive to temperature, while seston ionomes are largely shaped by temporal lake processes, with implications for nutrient dynamics and lake functioning under a warming climate.

TABLE OF CONTENTS

TABLE OF CONTENTS - CONTINUED

TABLE OF CONTENTS - CONTINUED

LIST OF TABLES

LIST OF FIGURES

LIST OF FIGURES – CONTINUED

LIST OF FIGURES – CONTINUED

LIST OF ABBREVIATIONS

Al	Aluminum
ANOVA	Analysis of variance
Ba	Barium
C	Carbon
Ca	Calcium
Cd	Cadmium
CLR	Centered log-ratio
Co	Cobalt
Cr	Chromium
Fe	Iron
GRH	Growth Rate Hypothesis
K	Potassium
MANOVA	Multivariate analysis of variance
Mg	Magnesium
Mn	Manganese
Mo	Molybdenum
N	Nitrogen
Na	Sodium
P	Phosphorus
PCA	Principle component analysis
PEG	Phytoplankton Ecology Group
S	Sulfur
Si	Silicon
Sr	Strontium
Zn	Zinc

CHAPTER 1: TEMPORAL CHANGES IN ZOOPLANKTON ELEMENTAL COMPOSITION IN A EUTROPHIC, DIMICTIC LAKE

INTRODUCTION

Anthropogenic nutrient loading is one of the greatest threats to the health of lake ecosystems (Carpenter et al., 1998), resulting in accelerated rates of eutrophication in lentic systems that are driven by intensification of agriculture and expansion of urbanization (Carpenter et al., 1998; Schindler et al., 2016; Paerl et al., 2016; Wurtsbaugh et al., 2019). Eutrophication can cause harmful cyanobacterial blooms (Schindler et al., 2012; Schindler et al., 2016), create hypoxic zones (Vitousek et al., 1997; Paerl et al., 2016), and alter composition and structure of biological communities (Wetzel, 2001; Wurtsbaugh et al., 2019).

Aquatic organisms are sensitive to fluctuations in water chemistry and nutrient concentrations. Particularly, total nitrogen (N) and phosphorus (P) concentrations often shape food webs and community composition (Kelly et al., 2024). Seston, the suspended matter that includes phytoplankton, can be used as a measure of resource food quality for freshwater primary consumers. The elemental composition of seston is highly plastic and often reflects environmental nutrient conditions (Elser, 2001; Sterner & Elser, 2002). However, zooplankton have a more constrained elemental composition (Sterner & Elser, 2002) which can create elemental imbalances between trophic levels that can impact their growth and productivity (Sterner & Elser, 2002; Acharya et al., 2004).

Ecological Stoichiometry

Ecological stoichiometry provides a robust framework for understanding how variations in elemental concentrations affect organismal physiology across different trophic levels (Sterner & Elser, 2002). This framework incorporates key principles, such as Proust's law of definite proportions, that states that a pure compound will contain the same relative amount of elemental constituents regardless of source and preparation; as well as the law of conservation of mass, which states that matter is neither created nor destroyed, only transformed. In the context of ecological stoichiometry, these laws allow us to form predictions based on the proportions of elements in chemical reactions and their products (Sterner & Elser, 2002). Through this approach, there is potential to track elements and assess the effects of nutrients as they move through organisms and the environment (Frost et al., 2005; Hessen et al., 2013; Wagner et al., 2013).

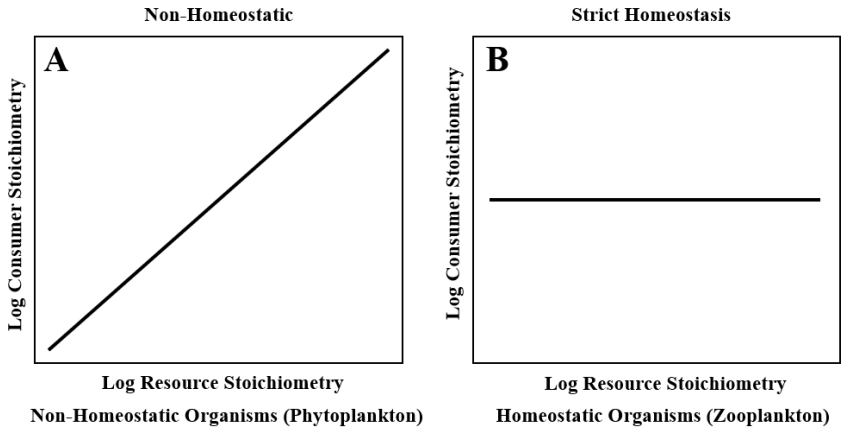

Figure 1.1. Homeostatic differences of element content, relating consumer stoichiometry to food resource stoichiometry. Depicted is a non-homeostatic (A) and a strict homeostatic pattern (B).

A central concept in ecological stoichiometry is homeostasis, defined as limited variation in chemical composition within an organism compared to its food resource.

Organisms regulate many internal processes to maintain homeostasis, in terms of uptake, assimilation, and excretion (Sterner & Elser, 2002). Concerning elemental composition, homeostasis allows organisms to maintain a relatively constant chemical composition by adjusting internal elemental ratios, regardless of the organism's food resource composition (Frost et al., 2005). However, homeostatic strength varies greatly by trophic level (Frost et al., 2005; Persson et al., 2010), allowing differential analysis of physiological characteristics between organisms, such as consumers and producers.

Autotrophs, like phytoplankton, exhibit non-homeostatic responses to variation in environmental elemental supplies, leading to variable elemental biomass ratios (Fig 1.1A). Phytoplankton are highly influenced by nutrient availability, leading to inconsistent elemental compositions that often reflect environmental nutrient levels (i.e. you are what you eat; Sterner & Elser, 2002). In contrast, consumers, such as zooplankton, tend to be more homeostatic and exhibit relatively less variability in their internal element concentrations (Fig 1.1B; Sterner & Elser, 2002). Thus, primary consumers are often challenged with nutritional imbalances stemming from highly plastic food resource composition, and more constrained elemental composition within their own bodies. While consumers can overcome minor nutritional imbalances by altering their feeding behavior and assimilation, larger nutritional imbalances can adversely affect consumer population growth and reproductive rates (Sterner & Elser, 2002). For example, when fed algae varying in C:P ratios, *Daphnia* can maintain a relatively homeostatic P composition at the cost of reduced growth (Sterner et al., 1993; DeMott et al., 1998; Wagner & Frost, 2012).

Another fundamental concept in ecological stoichiometry is the Growth Rate Hypothesis (GRH), which provides an explanation for variations in elemental composition among different taxa (Elser et al., 2000). The GRH mechanistically links ecological stoichiometry to integrated physiology, cell biology, and growth in relation to available food sources. Biological components such as lipids, proteins, and RNA vary interspecifically due to differences in organismal physiology and life history (Elser et al., 1996). Within invertebrates, biochemical allocation offers insight into the elemental composition of an organism, as these biomolecules are correlated with carbon (C), N, and P composition, with lipids being primarily C-based, proteins being rich in N, and RNA as a P-rich biomolecule. This tripartite relationship between elements, biomolecules, and growth forms the foundation of the GRH. This framework led to the prediction that organisms with faster growth rates have higher P content, due to the need for P-rich ribosomal RNA, which is a necessary component for protein synthesis and growth (Elser et al., 1996, 2001). Laboratory studies have used the GRH to demonstrate how the elemental content of food resources influences consumer growth, such as food P content positively correlating to *Daphnia* growth (Urabe & Watanabe 1992; Sterner et al., 1993; Acharya et al., 2004). By linking cellular biochemistry to trophic interactions, the GRH has broad ecosystem-wide implications, including nutrient cycling, community composition, and food web dynamics (Sterner & Elser, 2002).

Physiological differences between Daphnia and copepods

Crustacean zooplankton, such as cladocerans and copepods, are common freshwater taxa and form a link between primary production and higher trophic levels.

While these two taxa co-occur and dominate freshwater systems, they differ in physiology, life history traits, and elemental composition.

Cladocerans, such as *Daphnia*, consume a wide range of particles, including phytoplankton and detritus. The particles they consume depends on the size of the individual but can reach up to 60μm in size (Burns, 1968; Allan, 1976; Geller & Müller, 1981; Sommer & Sommer, 2006). Due to the morphology of their filtering apparatus, *Daphnia* are unable to selectively feed, leading them to ingest both high-quality and low-quality food (Lampert, 1987). Despite this limitation, daphnids can detect and aggregate in areas with high abundance of food (Leibold, 1990; Sterner & Schwalbach, 2001; Jensen et al., 2001). Due to high feeding efficiency and fast generation times facilitated by parthenogenesis, *Daphnia* can potentially deplete available resources and apply strong top-down control on phytoplankton communities (Becker et al., 2004).

According to the GRH, organisms with high growth rates require more P for ribosomal RNA and protein synthesis (Elser et al., 2000; Elser et al., 2003). As a result, *Daphnia* often maintain relatively constant, low C:P and N:P ratios, and have shown relatively strong stoichiometric homeostasis under lab conditions (Hessen & Lyche, 1991; Sterner & Elser, 2002). Daphnids with a high P demand can also affect seston nutrient composition by retaining P within their bodies, causing seston C:P to increase (Elser & Urabe, 1999).

Work that has focused on copepod physiology and stoichiometry has mostly been conducted with marine species. Freshwater copepods are generally smaller and less abundant than marine species and inhabit a more variable environment that is

characterized by seasonal fluctuations in temperature, nutrient availability, and food quality (Sterner & Elser, 2002). These ecological distinctions can lead to different stoichiometric profiles (Andersen & Hessen, 1991). For instance, freshwater copepods tend to have higher C:N, C:P, and N:P ratios than marine species, reflecting differences in life-history traits among copepod taxa (Downing, 1997; Herstoff et al., 2023). Additionally, while studies on copepods have examined stoichiometric variation across ontogeny (Carillo et al., 2001; Meunier et al., 2016; Malzahn et al., 2016; Mathews et al., 2018), habitat type (Herstoff et al., 2023), and latitude (Herstoff et al., 2023), little research has been done on how copepod elemental composition changes temporally, in situ. Similarly, while some research has assessed how copepods influence seston stoichiometry (Urabe, 1995), fewer studies have directly examined changes in the copepod elemental composition itself and with relation to environmental variability in freshwater lakes.

In contrast to *Daphnia*, copepods exhibit greater selectivity in feeding behavior. While many cyclopoid copepods are predaceous, others selectively feed on prey based on size (Allan, 1976), motility (Tiselius & Jonsson, 1990), or elemental composition (DeMott 1986; Cowles et al., 1988; Sommer & Sommer, 2006). Unlike *Daphnia*, copepods have the ability to reject food items that are unpalatable (Geller & Müller, 1981), mitigating elemental limitations, and allowing preferential consumption of higher quality food (Sommer & Sommer et al., 2006). This selectivity provides copepods with the ability to decrease the elemental imbalances between their own body stoichiometry and seston resource quality. However, their longer generation times, slower growth rates

as adults, and greater investment in structural tissues such as chitin, contribute to their higher N content compared to daphnids (Andersen & Hessen, 1991; Sterner & Elser, 2002). As a result, their grazing pressure on seston is often weaker or more variable than that of daphnids (Sommer & Sommer, 2006). In some lakes, copepod predation may even promote small phytoplankton growth, through their release during consumption of heterotrophic protists, thereby indirectly altering seston composition in unexpected ways (Sommer & Sommer, 2006). Similar to some daphnids, many copepod species overwinter as adults (Allan, 1976; Barth-Jensen et al., 2022) or enter diapause over winter months, allowing them to emerge earlier in the season and take advantage of spring phytoplankton blooms (Allan, 1976; Adrian et al., 2006).

In summary, the physiological and life history distinctions between *Daphnia* and copepods translate into distinct stoichiometric profiles and ecological roles. *Daphnia* may have stronger consumer-driven nutrient recycling of P due to their rapid growth and high P demand (Acharya et al., 2004), whereas copepods may influence N dynamics more due to their selective feeding and higher N demand (Allan, 1976; Becker et al., 2004). Assessing differences in elemental composition, abundance, and environmental responsiveness between these two taxa can provide more understanding for how zooplankton community structure affects biogeochemical processes within the same system (Elser & Urabe, 1999; Sterner & Elser, 2002). Because *Daphnia* and copepods co-occur in many freshwater lakes, high frequency monitoring of their stoichiometry, biomass, and abundance can provide important insight into lake processing and seasonal trophic level interactions.

AIMS

Here, we will answer what are the major drivers of zooplankton elemental composition? We hypothesize (1) phytoplankton elemental composition will not significantly impact zooplankton elemental stoichiometry, because zooplankton elemental composition is relatively homeostatic, displaying minimal plasticity with large changes in food quality (Acharya et al., 2004; Frost et al., 2005). Moreover, we hypothesize that (2) temperature will alter the elemental composition of each zooplankton taxa (Somero, 2004; Wojewodzic et al., 2011a; Prater et al., 2018). We predict that zooplankton will have lower %C due to increased metabolic rates at higher temperatures, as well as lower %P due to ribosomal RNA having greater efficiency under warm temperatures (Prater et al., 2018). Furthermore, we hypothesize that (3) zooplankton stoichiometric profiles will differ interspecifically and on a temporal scale due to variation in life-history traits and biochemical allocation (Allan, 1976; Elser et al., 1996). We predict that *Daphnia* will have a higher P content compared to copepods due to the faster growth rates of cladocerans (Andersen & Hessen, 1991; Elser et al., 1996; Urabe & Watanbe, 1992; Sterner et al., 2003; Acharya et al., 2004). Alternatively, we predict that copepods will have more %N required for chitinous exoskeletons (Andersen & Hessen, 1991; Sterner & Elser, 2002).

METHODS

Study site: Seven Ponds Nature Center – Tree Top Pond

We sampled zooplankton and seston from a temperate, eutrophic lake located in Dryden, MI (USA). Tree Top Pond is a dimictic lake within Seven Ponds Nature Center,

with a surface area of 15,161.56m^2, a max depth of 11m, and a total volume of 24,258m^3 (24,258,000L). Land use is dominated by forest (45.61%), woody wetlands (19.43%), pasture (15.38%), cultivated crops (7.17%), and developed land (5.68%) (Stroud Water Research Center, 2017).

Field sampling

To examine the drivers of zooplankton elemental composition, we sampled seston and zooplankton weekly, beginning shortly after ice-off in March and continuing through September 2024. This time span is reflective of the average growing season in northern temperate lakes, as well as the seasonal plankton succession pattern (Sommer et al., 1986; Prater et al., 2018). At the deepest part of the lake, we collected water from various depths to analyze particulate concentrations of nutrients and chlorophyll *a*. During isothermal conditions, we collected whole water samples using a Van Dorn sampler from the surface and at 5m and 9m depth. At the onset of stratification, we collected samples every meter from the surface to 9m. All water samples were stored in acid-washed 2L bottles on ice, until they were processed in the lab.

In addition to weekly sampling, we had a buoy anchored in the center of Tree Top Pond with eight sensors (HOBO, Onset), spanning the surface to 9.3m, that recorded temperature every 15 minutes, which was used to determine the weekly average water column temperature.

To collect zooplankton, we performed three quantitative zooplankton biomass samples by making three fixed-depth (8m) vertical tows with a 64µm zooplankton net

(30cm diameter, 90cm long). These samples were rinsed into 1L dark bottles and kept on ice for transport to the lab. Additionally, numerous tows (5-15) were sampled and stored in a 2L bottle in order to collect sufficient zooplankton biomass to determine their elemental composition.

Sample processing

Once the samples were returned to the laboratory, we filtered a known volume of water from all depths onto ashed 0.7µm glass fiber filters for particulate C, N, P, and chlorophyll *a* analysis. All filters were labeled and stored at -20°C until processing.

Triplicate zooplankton quantitative tows were concentrated to 135mL of lake water. Each tow was preserved with 4% formalin, buffered with 0.12M sucrose (Haney and Hall, 1973; Dumont et al., 1975; Bottrell et al., 1976) and placed in a plastic storage container for future analysis.

Zooplankton collected for body C, N, and P content were separated by daphnids and copepods and pooled into separate samples. Only live animals were sampled and preserved in order to maintain molecular and elemental composition without leaching. In order to slow down the zooplankton for collection, we placed a subsample of zooplankton into a plastic container with ¼ of an Alka-Seltzer tab. Using a plastic pipette, we collected ~0.5 – 1 mg dry mass (~10-25 daphnids, or 15-30 copepods) to determine the animal's C, N, (n=5), and P (n=5) content. Samples saved for CN were placed into pre-weighed tin boats and samples for P were placed into aluminum boats. All samples were dried at 60°C for 24h and then placed into a desiccator until processing.

Seston C, N, P and chlorophyll a analysis

Particulate P filters were placed in glass vials and digested using a hot 1.65% potassium persulfate solution as previously described (Wagner & Frost, 2012; Prater et al., 2018). P concentrations were analyzed using molybdate-blue ascorbic acid colorimetry and absorbance spectroscopy, using either a 1 or 5cm pathlength depending on the expected concentration (APHA, 1992). Particulate CN filters were dried at 60°C for 24h prior to analysis on a Costech 4010 elemental analyzer as previously described (Wagner & Frost 2012).

Chlorophyll *a* filters were extracted in 90% acetone for 24h at -20°C. We calculated the concentration of chlorophyll *a* using the EPA 445.0 method using fluorescence and the chlorophyll-acid module (Turner Design; Arar & Collins, 1997).

Zooplankton C, N, and P analysis

The dried daphnid and copepod CN samples contained within tin cups were weighed to the nearest 1µg on a microbalance (RADWAG MYA 5.5 Y.F.A) prior to analysis. The %C and %N content was analyzed on a Costech 4010 as previously described (Prater et al., 2018; Wagner & Frost, 2012). We analyzed daphnid and copepod P content by weighing organisms to the nearest 1µg on a microbalance and placing them in a glass vial. Prior to P analysis, the samples were combusted at 450°C for 3h and allowed to cool to room temperature. The daphnid and copepod P samples were oxidized in a hot 1.65% potassium persulfate solution and measured using the molybdate-blue ascorbic acid colorimetry and absorbance spectroscopy (APHA, 1992).

Zooplankton Abundance and Biomass

Zooplankton biomass estimates were conducted using each quantitative tow replicate (n=3). The volume filtered of each tow is found using the volume of a cylinder:

$$V = \pi r^2 h \quad (1)$$

where r is the radius of the zooplankton net (0.3m diameter; 0.15m radius) and h is the height of each tow (8m). Thus, each tow replicate filtered through ~565L of water. For each replicate tow, we subsampled 1mL and loaded it on a Sedgewick-Rafter slide. Zooplankton were counted on an inverted microscope (VWR) at 40x magnification and measured using the Moticonnect digital photo software. We measured a minimum of 20 *Daphnia*, cyclopoid copepods, and calanoid copepods per replicate, or a maximum of 7 slides per replicate. *Daphnia* were measured from the anterior edge of eye to the base of the tail (Figure 1.2A). Calanoid and cyclopoid copepods were measured from the anterior edge of the cephalosome to the base of the caudal rami of the urosome (Figure 1.2B and 1.2C) (Culver et al., 1985).

To calculate biomass estimates, we used taxa-specific length-weight regression conversion equations, as follows:

$$W = \alpha L^{\beta} \quad (2)$$

where W = dry weight in μg, L = length in mm, β is a scaling factor that relates a 3-dimensial animal's mass to length, and α is the mass of an organism proportional to its length (Watkins et al., 2011; Burgess et al., 2015). For each tow, mean body length (± standard deviation) was calculated for each taxon, and the corresponding regression was applied to estimate individual biomass (Table 1.1). Average biomass per individual was

then multiplied by the total number of organisms per sample to estimate sample-based biomass.

To standardize densities, zooplankton counts and biomass were first expressed as organisms/mL and µg/mL. These values were corrected to account for preservation volume, yielding density based on lake water volume only. We then scaled up the biomass and abundance to the total lake water volume that was filtered by each tow (Equation 1). Biomass and abundance per L were derived by dividing the corrected sample biomass and organism counts by the calculated tow volume (L).

Error propagation was incorporated into the biomass and abundance calculations in two steps. First, the standard deviation of individual lengths was carried through the length-weight regressions to provide uncertainty in biomass estimates. Second, variation between replicate tows for each sampling date and taxa was calculated as mean ± standard deviation of abundance and biomass per L. This approach allowed us to show both measurement error (within-sample length variation) and sampling variability (within replicate tows).

Table 1.1. Length-weight coefficients for zooplankton taxa and their sources.

Organism	α	β	Notes	Reference
Daphnids	1.47	2.83	0.6-4.0mm	Bottrell et al., 1976
Calanoid copepods	1.53	2.59		Burgess et al., 2015
Cyclopoid copepods	1.66	3.97	0.3-1.5mm $r^2 = 0.97$	Rosen et al., 1981

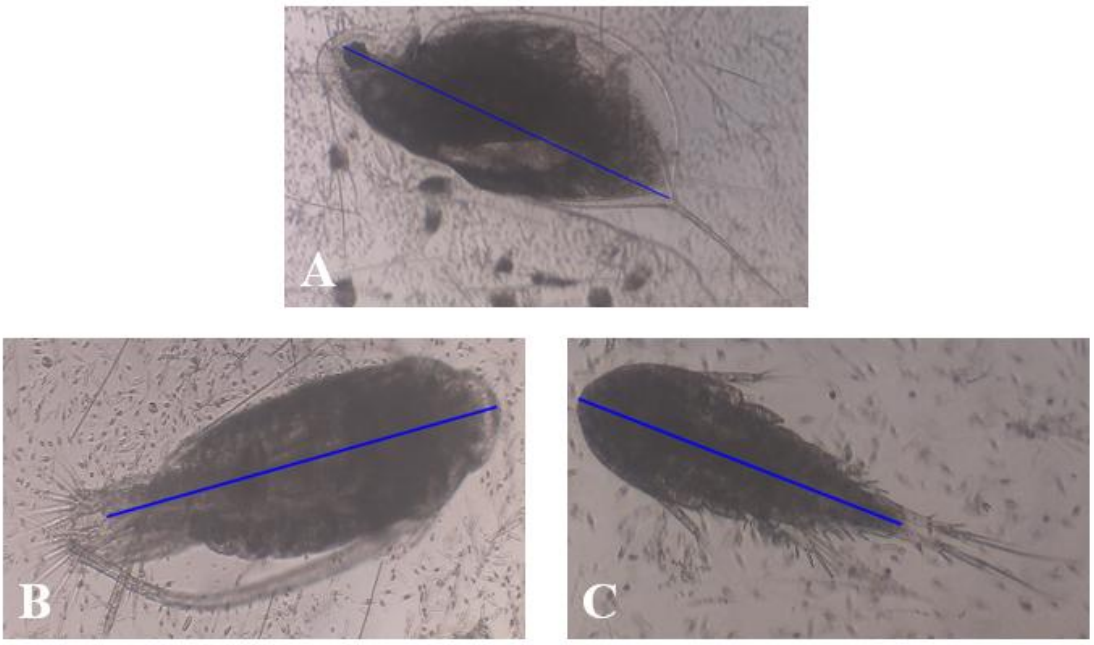

Figure 1.2. Photographs of zooplankton on inverted microscope using Moticonnect software. Each zooplankton taxa is shown with a blue line to indicate measurement distance, for *Daphnia* (A), calanoid copepods (B), and cyclopoid copepods (C).

Statistical analysis

All statistical analyses were completed in R using version 4.4.1 (R core Team, 2023). All regression analyses were visually inspected and examined for autocorrelation using the acf() function. Model assumptions and diagnostics were checked using the performance package (Lüdecke et al. 2021). Prior to all analyses, we averaged our analytical replicates of zooplankton and seston elemental composition.

To test hypothesis 1, that examines the correlations between seston and zooplankton elemental composition, we fit linear regressions between zooplankton and seston ratios (C:N, N:P, C:P) using the lm() function. We then conducted additional regressions between zooplankton elemental percentages (%C, %N, %P) and seston ratios

to explore further relationships. Because zooplankton can eat from various depths, the seston data were averaged from 0-8m depth to match the zooplankton sampling depth. A significant regression would suggest that food stoichiometry contributed to variation in zooplankton elemental composition.

For hypothesis 2, that investigates the relationships between zooplankton elemental content and temperature, we followed the same approach: regressing weekly average temperature (0-8m) against zooplankton ratios and elemental percentages for each taxon. Here, the independent variable was weekly average temperature, and the dependent variable was zooplankton elemental composition. A significant regression would indicate that the elemental composition of *Daphnia* or copepods is dependent on temperature. Finally, we regressed the residuals from the temperature-zooplankton elemental percentage regressions against seston elemental ratios to test whether seston explained variation after accounting for temperature effects. We then performed the inverse analysis, regressing residuals from the seston-zooplankton elemental percentages regressions against temperature. A significant regression between the residuals of one analysis (e.g. temperature) and the other variable (i.e. seston stoichiometry) indicates that variation not explained by the first model can be attributed to the second variable.

To test hypothesis 3, that zooplankton elemental compositions will differ interspecifically between taxa, we conducted a two-way ANOVA with month and taxon as factors, followed by Tukey's post-hoc analysis.

RESULTS

Average water temperature and seston elemental ratios varied temporally (Fig 1.3). The average water temperature across our 0-8m sampling range extended from 5°C in early March and increased until the end of July, reaching a peak of 18°C, and subsequently decreased through the end of September (Fig 1.3A). In March, seston C:N ratios were ~7 but increased to mid-July peak of ~10 (Fig 1.3B; coefficient of variation, c.v = 10%). N:P ratios also increased over the sampling period, starting near 20 in March and reaching a maximum of ~35 by late September (Fig 1.3C; c.v = 16%). Seston C:P ratios showed the greatest variability, beginning at ~150 early in March and reaching ~300 in July (Fig 1.3D; c.v. = 23%).

Zooplankton abundance and biomass varied across the sampling season (Fig 1.4). Shortly after ice-off, the zooplankton community was dominated by cyclopoid copepods, reaching peak densities of ~30 individuals/L in April and May, before declining and converging with *Daphnia* and calanoid copepods (<10 individuals/L; Fig 1.4A). Calanoid copepods remained low in abundance (<5 individuals/L) from March through September, whereas *Daphnia* were initially scarce (<2 individuals/L) in March and April but reached peak abundance in May, ranging between 5-10 individuals/L. Biomass patterns followed similar trends, with cyclopoid copepods dominating early in the season (~5-15 µg/L) before declining by mid-summer (Fig 1.4B). Calanoid copepod biomass remained low (<5 µg/L) throughout the entire sampling period. *Daphnia* biomass had two distinct peaks, in May and August, with biomass reaching ~5 µg/L.

The elemental composition of the seston, used here as a proxy for food resource stoichiometry, showed inconsistent relationships with zooplankton elemental compositions, with effects that were both taxon-specific and element-dependent (Table 1.2, Fig 1.5). We observed a negative correlation between copepod C:N and seston C:N (Fig 1.5A; Table 1.2). Additionally, *Daphnia* N:P was positively correlated with seston N:P (Fig 1.5B; Table 1.2). However, we found no correlation between zooplankton C:P and seston C:P for either taxon (Fig 1.5C; Table 1.2).

Similarly, zooplankton elemental percentage correlations with seston stoichiometry were variable between taxon and element (Fig 1.6, Table 1.2). We found negative relationships between daphnid and copepod %C body content and seston C:N, N:P, and C:P (Fig 1.6A, B, C). Alternatively, only *Daphnia* %N was negatively correlated with seston C:N, N:P, and C:P ratios (Fig 1.6D, E, F). For %P, both taxa had negative correlations with C:N (Fig 1.6H) and C:P (Fig 1.6J). In contrast, only *Daphnia* %P body content negatively correlated with seston N:P ratios (Fig 1.6I).

Temperature was a significant predictor of elemental composition in zooplankton, but the magnitude of this effect varied by taxon and by element (Fig 1.7; Table 1.3). We found that *Daphnia* and copepod C:N ratios were negatively correlated with temperature (Fig 1.7A). Body N:P ratios for both *Daphnia* and copepods were positively correlated with temperature (Fig 1.7B). In contrast, only *Daphnia* C:P demonstrated a positive correlation with temperature (Fig 1.7C).

The relationship between zooplankton body elemental percentages and temperature was taxa and element dependent (Fig 1.8, Table 1.3). Both *Daphnia* and

copepods showed a significant negative relationship between %C and temperature (Fig 1.8A). In contrast, daphnid %N content negatively correlated with temperature (Fig 1.8B). Alternatively, both taxa had negative correlations between temperature and body %P content (Fig 1.8C).

Next, we tested whether residual variation in the relationships between zooplankton percent element content and seston stoichiometry could be explained by temperature (Fig 1.9 & Fig 1.10; Table 1.4). For *Daphnia*, residuals from %C content regressions with seston C:N, N:P, and C:P ratios were negatively correlated with temperature (Fig 1.9). The residuals from the *Daphnia* %N content and seston C:N had a negative relationship with temperature. Finally, the residuals of daphnid %P and seston C:N, N:P, and C:P were negatively correlated with temperature. In contrast, the only relationship observed for copepods was the residuals between %C and seston C:N, which had a negative relationship with temperature (Fig 1.10).

We found that zooplankton body %C, %N, and %P content were significantly affected by month, taxon, and the interaction between month and taxa (Figure 1.11; Table 1.5). In spring (March to May), *Daphnia* and copepods had similar C content (~50-55%), which diverged over the season, to ~40% and ~45%, respectively. *Daphnia* and copepod %N remained relatively constant through the sampling period, while *Daphnia* had consistently lower %N (~9-11%) than copepods (~11-12%). P content was highest in *Daphnia* during the early spring (~1.8%) which was significantly higher than copepod %P (~1.3%). However, the gap between the %P content of each taxon

diminished during the summer, that by late summer (July to September), the %P content of each taxon converged and was not significantly different (~1.0-1.2%).

Table 1.2. Linear regression results correlating zooplankton elemental composition to seston stoichiometry, including the regression equation, adjusted r^2, F-values, and p-values. Significant regressions ($p<0.05$) are shown in bold. Degrees of freedom (df) are written as numerator, denominator.

Taxon	Response	Predictor	Regression equation	r^2	F-value (1, 26)	p-value
Daphnia	%C	Seston C:N	y = – 2.75x + 63.61	0.16	6.06	**0.02**
Copepod			y = – 1.56x + 58.84	0.13	4.86	**0.04**
Daphnia	%C	Seston N:P	y = -0.84x + 65.39	0.58	39.02	**<0.001**
Copepod			y = -0.48x + 59.85	0.48	25.97	**<0.001**
Daphnia	%C	Seston C:P	y = -0.07 + 57.68	0.53	30.97	**<0.001**
Copepod			y = -0.04x + 55.55	0.44	22.26	**<0.001**
Daphnia	%N	Seston C:N	y = -0.50x + 13.01	0.17	6.46	**0.017**
Copepod			y = 0.03x + 10.98	-0.04	0.04	0.85
Daphnia	%N	Seston N:P	y = – 0.11x + 12.17	0.29	12.31	**0.002**
Copepod			y = – 0.008x + 11.4	-0.03	0.12	0.73
Daphnia	%N	Seston C:P	y = -0.01x + 11.39	0.34	14.77	**<0.001**
Copepod			y = -0.0004x + 11.27	-0.04	0.04	0.84
Daphnia	%P	Seston C:N	y = -0.14x + 2.41	0.21	8.14	**0.008**
Copepod			y = -0.07x + 1.73	0.29	12.13	**0.002**
Daphnia	%P	Seston N:P	y = -0.03x + 2.31	0.51	28.57	**<0.001**
Copepod			y = -0.008x + 1.39	0.06	3.93	0.058
Daphnia	%P	Seston C:P	y = – 0.003x + 2.02	0.49	27.35	**<0.001**
Copepod			y = – 0.001x + 1.38	0.22	8.69	**0.007**
Daphnia	C:N	Seston C:N	y = – 0.05x + 5.83	-0.02	0.51	0.48
Copepod			y = – 0.18x + 6.28	0.14	5.24	**0.03**
Daphnia	N:P	Seston N:P	y = 0.17x + 10.28	0.37	16.66	**<0.001**
Copepod			y = 0.12x + 18.19	0.03	1.73	0.20
Daphnia	C:P	Seston C:P	y = 0.03x + 72.05	0.37	3.62	0.07
Copepod			y = 0.0005x + 0.01	-0.04	<0.001	0.98

Table 1.3. Linear regression of zooplankton elemental composition in response to temperature. Shown is each regression equation, adjusted r^2, F-values with degree of freedom shown as numerator, denominator, and p-values. Significant regressions ($p<0.05$) are shown in bold.

Taxon	Response	Predictor	Regression equation	df	r^2	F-value	p-value
Daphnia	%C	Temperature	y = – 0.94x + 55.75	1, 26	0.78	95.68	**<0.001**
Copepod			y = – 0.50x + 53.93		0.56	35.46	**<0.001**
Daphnia	%N	Temperature	y = – 0.13x + 11.04	1, 26	0.46	24.38	**<0.001**
Copepod			y = – 0.02x + 10.89		-0.004	0.88	0.36
Daphnia	%P	Temperature	y = – 0.003x + 1.98	1, 26	0.86	171.3	**<0.001**
Copepod			y = – 0.013x + 1.34		0.32	13.73	**0.001**
Daphnia	C:N	Temperature	y = – 0.04x + 5.99	1, 26	0.37	16.74	**<0.001**
Copepod			y = – 0.06x + 5.79		0.74	76.32	**<0.001**
Daphnia	N:P	Temperature	y = 0.22x + 11.87	1, 26	0.66	54.28	**<0.001**
Copepod			y = 0.26x + 17.78		0.30	12.38	**0.002**
Daphnia	C:P	Temperature	y = 0.63x + 71.58	1, 26	0.32	13.47	**0.001**
Copepod			y = 0.044x + 104.25		-0.04	0.012	0.91

Table 1.4. Summary of regression analyses examining the relationship between temperature and the residuals of zooplankton %carbon (C), %nitrogen (N), and %phosphorus (P), after accounting for seston stoichiometry (C:N, N:P, and C:P). Significant results indicate that temperature explained additional variation in zooplankton elemental composition not attributable to seston ratios.

Taxon	Response	Residuals used	Regression equation	r^2	F-value (1, 26)	p-value
Daphnia	%C	Seston C:N	y = -0.70x + 9.54	0.53	31.22	**<0.001**
Copepod			y = -0.37x + 4.97	0.34	15.18	**<0.001**
Daphnia	%C	Seston N:P	y = -0.27x + 3.71	0.14	5.23	**0.03**
Copepod			y = -0.12x + 1.66	0.03	1.95	0.17
Daphnia	%C	Seston C:P	y = -0.31x + 4.29	0.17	6.38	**0.02**
Copepod			y = -0.14x + 1.95	0.05	2.54	0.12
Daphnia	%N	Seston C:N	y = -0.09x + 1.19	0.25	9.81	**0.004**
Copepod			y = 0.02x – 0.26	-0.01	0.69	0.41
Daphnia	%N	Seston N:P	y = -0.04x + 0.59	0.05	2.33	0.14
Copepod			y = 0.03x – 0.38	0.02	1.56	0.22
Daphnia	%N	Seston C:P	y = -0.04x + 0.55	0.04	2.06	0.16
Copepod			y = 0.03x – 0.34	0.008	1.24	0.28
Daphnia	%P	Seston C:N	y = -0.03x + 0.43	0.60	41.1	**<0.001**
Copepod			y = -0.007x + 0.09	0.09	3.97	0.06
Daphnia	%P	Seston N:P	y = -0.02x + 0.22	0.22	8.68	**0.007**
Copepod			y = -0.007x + 0.09	0.07	2.88	0.10
Daphnia	%P	Seston C:P	y = -0.02x + 0.23	0.24	9.55	**0.005**
Copepod			y = -0.004x + 0.06	0.01	1.31	0.26

Table 1.5. Two-way analysis of variance (ANOVA) results for the influence of Month, Taxa, and their interaction on zooplankton %carbon (C), %nitrogen (N), and %phosphorus (P) content with the degrees of freedom (df), represented as numerator, denominator, F-values, and p-values.

ANOVA				
Response	**Predictor**	**df**	**F-value**	**p-value**
%C	Month	6, 42	28.84	**<0.001**
	Taxa	1, 42	67.62	**<0.001**
	Month x Taxa	6, 42	3.34	**0.008**
%N	Month	6, 42	6.49	**<0.001**
	Taxa	1, 42	227.20	**<0.001**
	Month x Taxa	6, 42	6.03	**<0.001**
%P	Month	6, 42	35.72	**<0.001**
	Taxa	1, 42	168.20	**<0.001**
	Month x Taxa	6, 42	12.25	**<0.001**

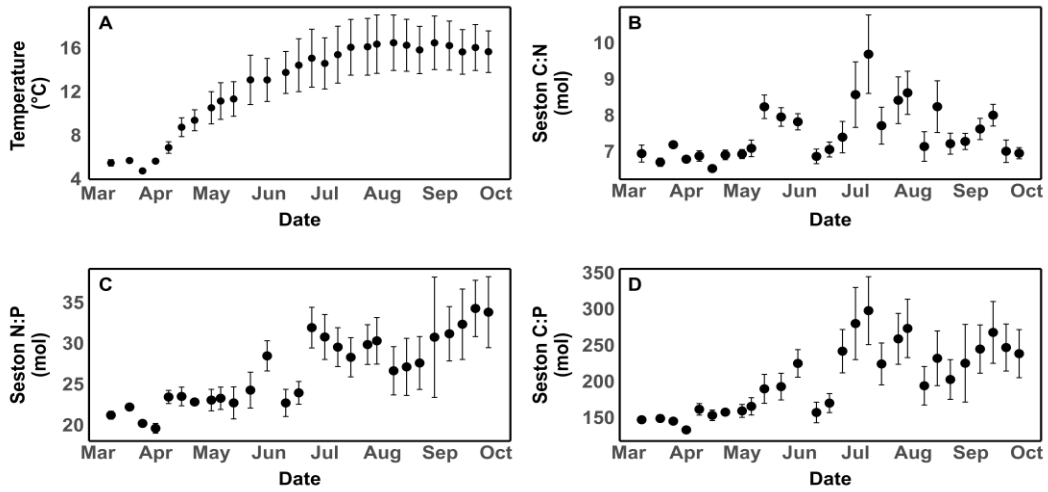

Figure 1.3. Seasonal variation in the average (± standard deviation) temperature of 0-8m (A) and average seston particulate molar ratios: carbon:nitrogen (C:N; mol; B), N:phosphorus (P; mol; C), and C:P (mol; D), ± standard deviation.

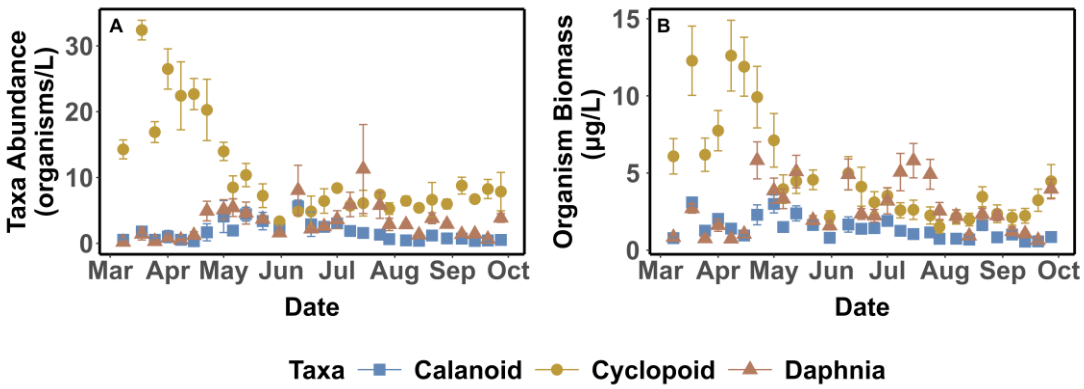

Figure 1.4. Abundance (A; individuals/L) and biomass (B; µg/L) for calanoid copepods (blue squares), cyclopoid copepods (yellow circles), and *Daphnia* (pink triangles) from March through September. Data points represent the average values for each sampling date for each taxon. Error bars indicate ± propagated standard error.

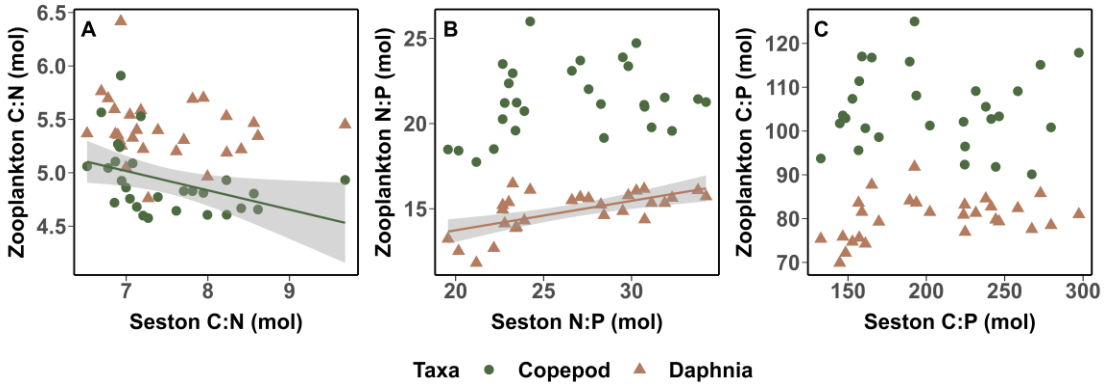

Figure 1.5. Copepod (green circles) and *Daphnia* (pink triangles) carbon:nitrogen (C:N mol; A), N:phosphorus (P mol; B), and C:P (mol; C) body content correlations with seston C:N (mol; A), N:P (mol; B), and C:P (mol; C). Significant regressions are denoted with regression lines, colored by taxa, with 95% confidence intervals in grey shading.

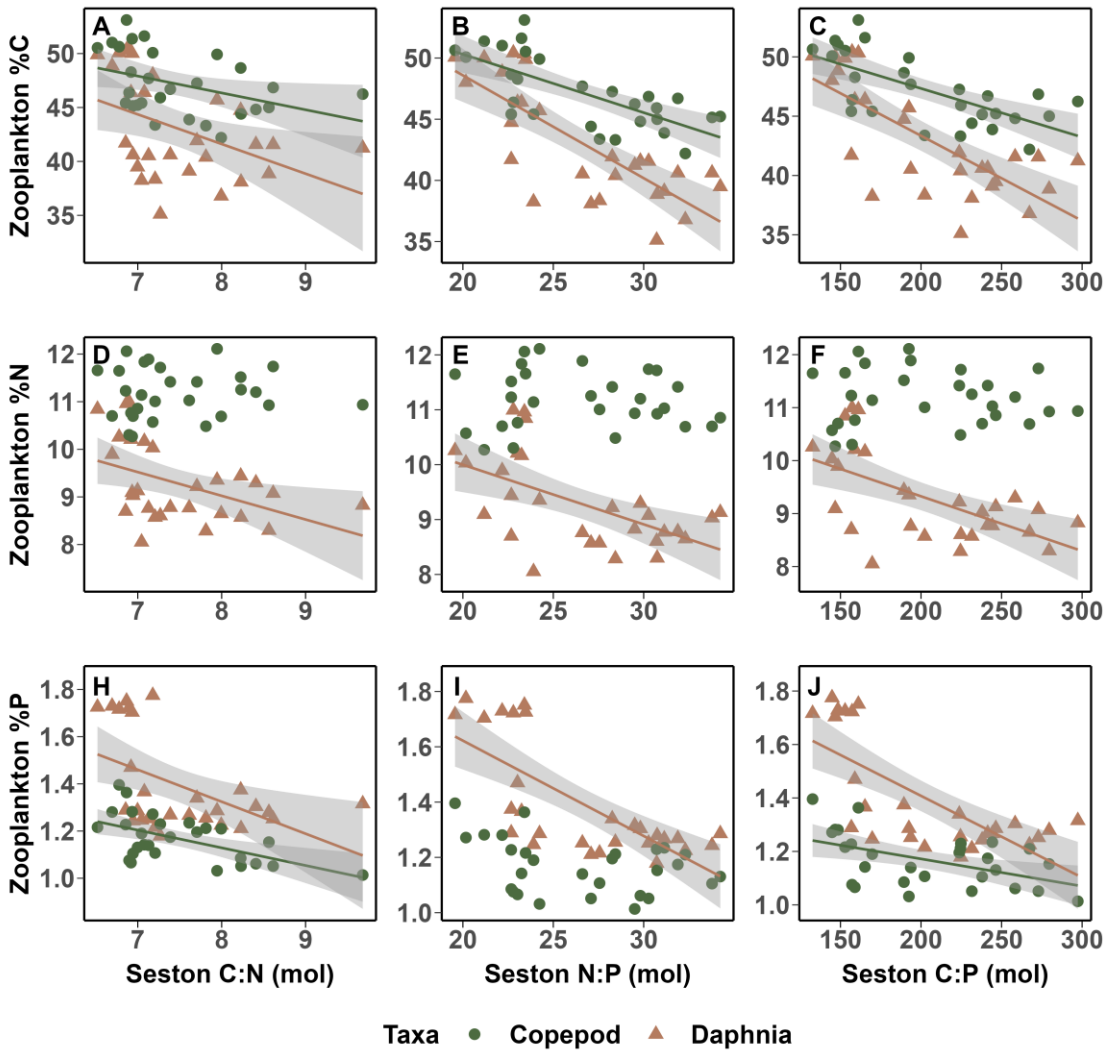

Figure 1.6. Percent carbon (%C; A, B, C), nitrogen (%N; D, E, F), and phosphorus (%P; H, I, J) body content for copepods (green circles) and *Daphnia* (pink triangles), correlated with seston C:N (A, D, H), N:P (B, E, I), and C:P (C, F, J). Regression lines indicate significant correlations with 95% confidence intervals shown in grey shading.

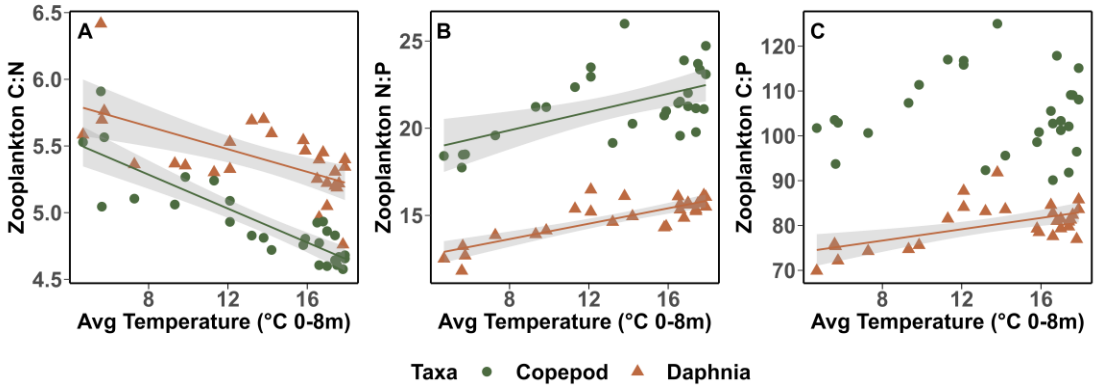

Figure 1.7. *Daphnia* (pink triangles) and copepod (green circles) carbon:nitrogen (C:N mol; A), N:phosphorus (P mol: B), and C:P (mol; C) plotted against the average temperature (°C) from 0-8m. Regressions lines are statistically significant relationships, with 95% confidence intervals shown in grey.

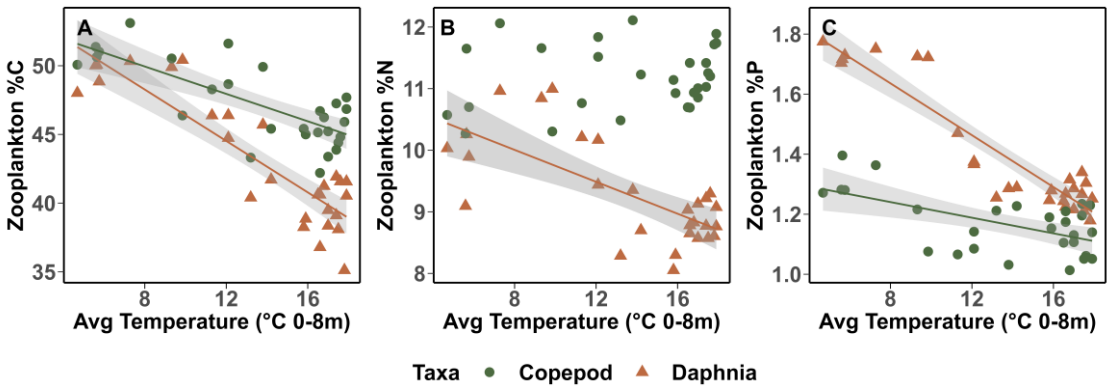

Figure 1.8. *Daphnia* (pink triangles) and copepod (green circles) body percent carbon (%C; A), nitrogen (%N; B) and phosphorus (%P) plotted against the average temperature (°C) from 0-8m. Regression lines indicate statistical significance ($p<0.05$), and shaded regions indicate 95% confidence intervals.

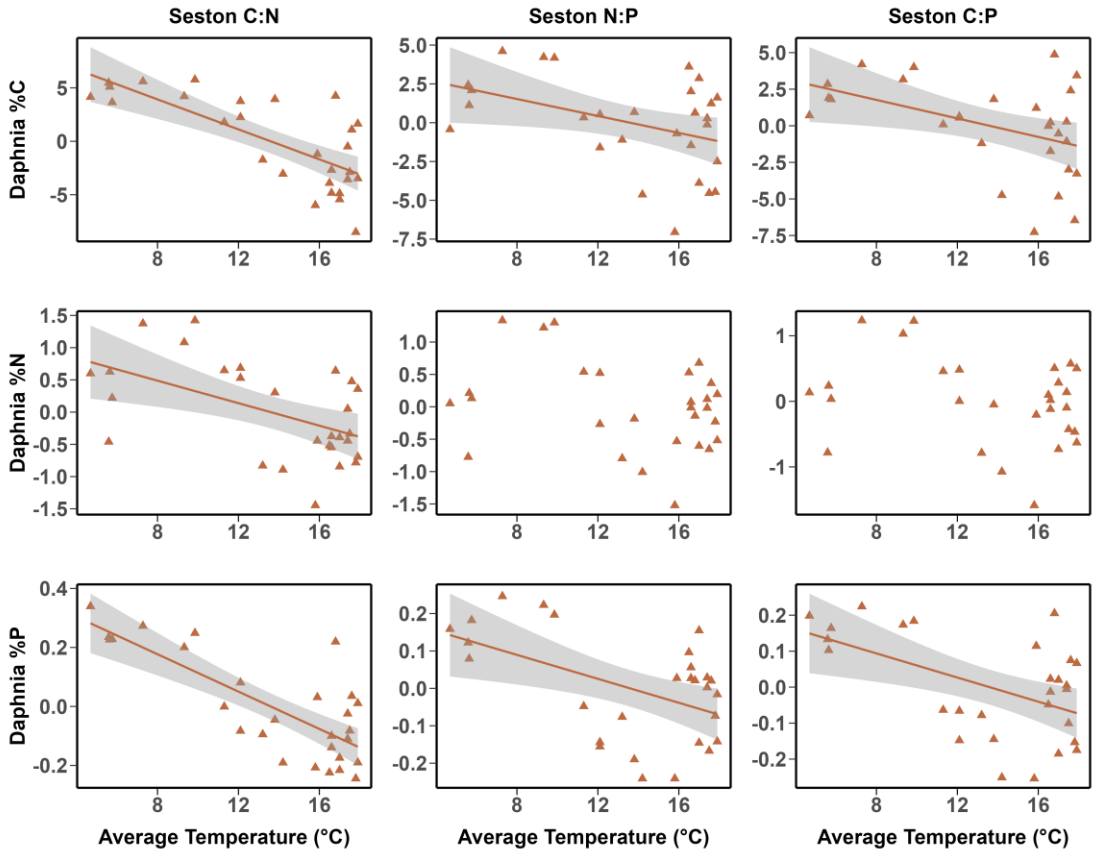

Figure 1.9. Residuals of the regressions between seston carbon:nitrogen (C:N mol; first column), N:phosphorus (N:P mol; second column), C:P (mol; third column) and *Daphnia* percent C (%C top row), %N (middle row), and %P (bottom row) regressed against the average 0-8m temperature (°C). Regression lines indicate a significant correlation, with shaded area indicating 95% confidence intervals.

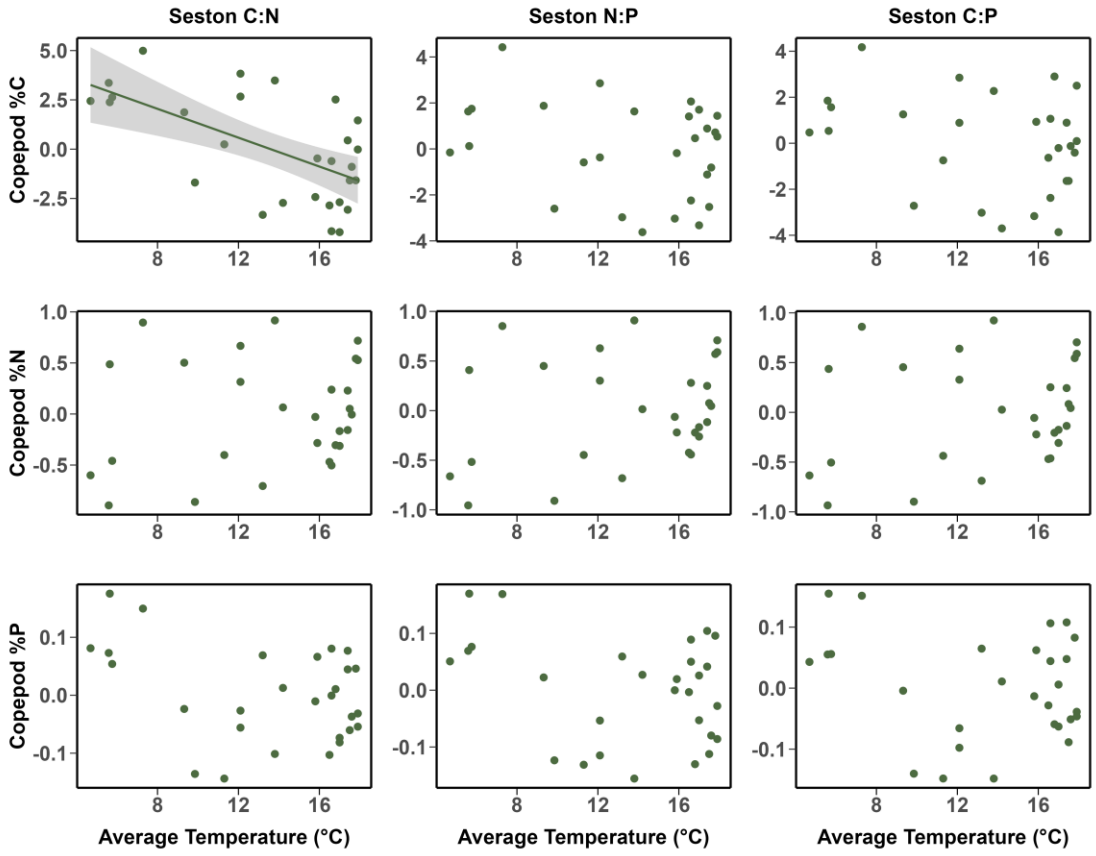

Figure 1.10. Residuals of the regressions between seston carbon:nitrogen (C:N mol; first column), N:phosphorus (N:P mol; second column), C:P (mol; third column) and copepod percent C (%C top row), %N (middle row), and %P (bottom row) regressed against the average 0-8m temperature (°C). Regression lines represent significant relationships, with shaded areas indicating 95% confidence intervals.

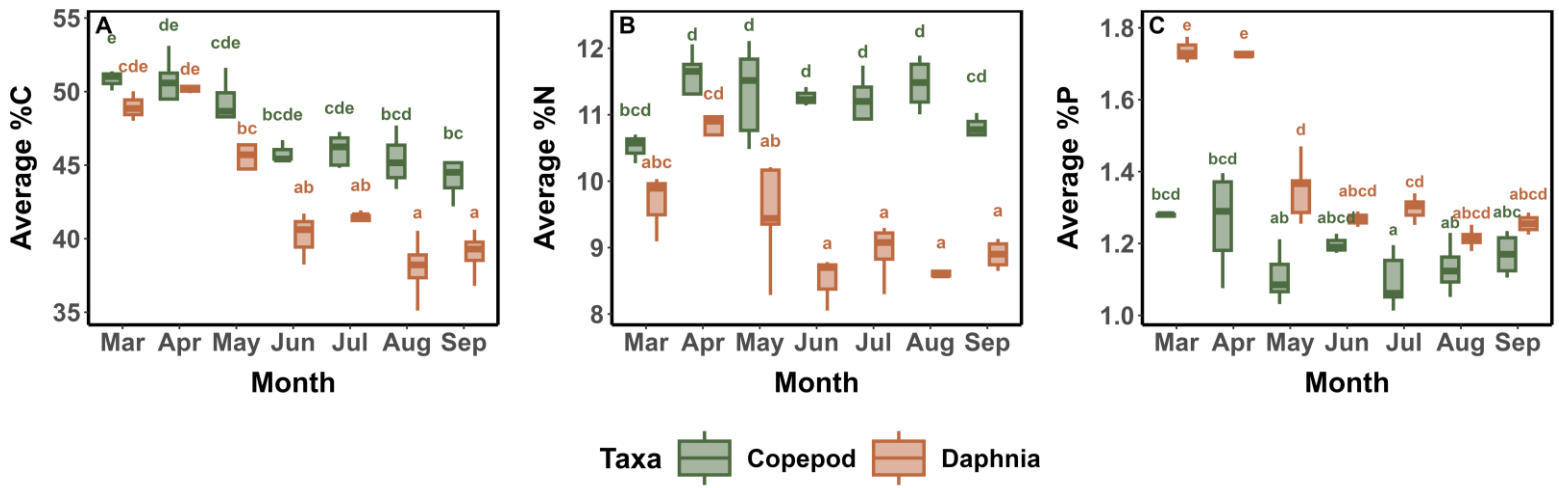

Figure 1.11. Seasonal change in elemental composition of *Daphnia* (pink) and copepods (green). Shown are %carbon (C; A), %nitrogen (N; B), and %phosphorus (P; C) starting in March and ending in September 2024. The box indicates the interquartile range, the horizontal line shows the median, with whiskers extending to 1.5x the interquartile range. Compact letters above each boxplot show statistical significance among groups based on post hoc comparisons.

DISCUSSION

Our study found that zooplankton elemental stoichiometry in Tree Top Pond was shaped by seston food quality and temperature, with genus-specific differences between taxa. Our results provide conflicting support for hypothesis 1, that the seston elemental composition will not affect zooplankton composition. While many of the body percent elemental contents negatively correlated with seston C:N, N:P, and C:P, the zooplankton C:N, N:P, and C:P ratios resulted in many non-significant relationships with seston elemental ratios. Further, we found support for hypothesis 2, that temperature would influence zooplankton elemental composition, specifically lowering %C and %P concentrations under increased temperature. The majority of daphnid and copepod ratios (i.e., C:N, N:P, C:P) and percent composition (i.e., %C, %N, and %P) varied with temperature. After the variation between seston elemental ratios and percent elemental content from *Daphnia* was accounted for, we found that the residual error for many of the elemental contents correlated with temperature. However, most of the residual variation between seston stoichiometry and copepod elemental content was not explained by temperature. We found partial support for hypothesis 3, that *Daphnia* and copepods differed in elemental profiles, with copepods exhibiting higher %N. Although %P content was initially different between the two taxa, by the end of the season, their %P content converged, suggesting that seasonal trends may mask interspecific elemental differences between taxa. Together, these findings highlight how zooplankton elemental composition is plastic in response to seston elemental composition and temperature.

There are numerous interspecific differences between *Daphnia* and copepods that may underline the patterns we observed. Our stoichiometric profiles were obtained from adults due to their size and ease of collection. *Daphnia* continue to grow throughout their life, with differences in growth rates (e.g., biomass accumulation), even after reproduction starts (Wagner & Frost 2012; Wagner et al. 2017) and maintain this growth through regular molting every 3-5 days (Ebert, 2005). In contrast, copepods do not molt once they reach adulthood and instead accumulate biomass via egg production (Hirst & McKinnon 2001). Both taxa can produce eggs at similar rates depending on the species and environmental conditions (Ewers, 1936; Gurney et al., 1990; McCauley et al., 1990). These differences in growth and allocation strategies are reflected in their elemental profiles, such as copepods consistently maintaining higher %N than daphnids, likely reflecting their greater investment in chitin-rich exoskeletons (Andersen & Hessen, 1991; Becker et al., 2004).

In partial support of hypothesis 1, we found zooplankton stoichiometry was not strongly correlated to seston stoichiometry, and there were more correlations with zooplankton stoichiometry and temperature than with seston food quality. Overall, food quality appeared to play a limited role in determining stoichiometric profiles, consistent with expectations of consumer homeostasis (Sterner & Elser, 2002; Acharya et al., 2004; Frost et al., 2005). With seston C:N and C:P ratios increasing temporally, we would expect zooplankton, especially *Daphnia,* to become P-limited (Urabe et al., 2003; Frost et al., 2006; Khattak et al. 2018) and have higher C:P ratios driven by increased %C. However, many of the relationships between zooplankton %C, %N, and %P and seston

stoichiometry were negative. For example, copepod C:N had a negative relationship with seston C:N ratio, primarily due to a decline in %C, while %N showed no significant relationship; thus, copepod C:N decreased with higher seston C:N ratios. Similarly, the positive correlation between seston and *Daphnia* N:P ratios was likely caused by a greater reduction in body P (33.5%) content compared to body N (26.7%) content. These findings resemble prior work showing that zooplankton maintain relatively stable elemental composition even under variable food conditions, with only certain elemental pools exhibiting plasticity (Acharya et al., 2004; Hessen et al., 2013).

Temperature showed more consistent effects on zooplankton stoichiometry. Zooplankton C:N and body %C content decreased with temperature. One explanation is that temperature influenced feeding rates and growth. For instance, *Daphnia* filtering rate can increase up to five times greater at 25°C relative to 15°C depending on the species (Burns, 1969). At colder temperatures, slower growth could result in greater assimilation of phytoplankton, leading to increased lipid content and higher %C (Wagner et al., 2015). As temperature increases, high growth rates may reduce lipid stores and increase metabolic rates, contributing to lower %C, as well as C:N and C:P (Hessen & Andersen, 2008; McFeeters & Frost, 2011; Wojewodzic et al. 2011a; Prater et al. 2018; Balseiro et al., 2021).

Phosphorus body content showed a different pattern, with %P converging between taxa as temperature increased, likely due to temperature's influence on ribosome efficiency (Wojewodzic et al., 2011b; Hessen et al., 2017). At higher temperatures, ribosomes operate more efficiently, reducing the cellular demand for ribosomes to sustain

growth, which in turn lowers body %P content (Prater et al., 2018; Balseiro et al., 2021). Although copepods generally invest less %P in P-rich biomolecules such as RNA and nucleic acids (Sterner & Elser, 2002; Hessen et al., 2013), we still found their %P declined with temperature. *Daphnia*, with typically faster growth rates than copepods, are expected to maintain higher %P (Elser et al., 2000, 2003; Acharya et al., 2004). Thus, the observed convergence in body %P suggests that P allocation to biomolecules must differ fundamentally between taxa (Andersen & Hessen, 1991; Sterner & Elser, 2002). Future studies should compare and contrast these differences in P allocation between these taxa at different temperatures using radioisotopes (Persson & Vrede, 2006; He & Wang, 2008).

Body N content also responded to warming, though in a taxon-specific way. Zooplankton N:P ratios increased with temperature, while *Daphnia* body %N content declined. Copepod %N, however, was largely invariable across seston C:N:P ratios and remained consistently higher than *Daphnia*. One explanation is that copepods, which do not molt as adults, invest more into N-rich chitin for their exoskeleton (Andersen & Hessen, 1991; Becker et al., 2004). Ribosome biochemistry may also link N and P responses, since ribosomes are ~15% N (Elser et al., 1996), so the increased efficiency of ribosomes at higher temperatures could lower %N and %P in daphnids. More broadly, these interspecific differences show how life-history traits shape elemental allocation and how seasonal conditions may modify stoichiometric divergence across taxa (Elser & Urabe, 1999; Villar-Argaiz et al., 2002; Sterner & Elser, 2002).

Our results indicate that zooplankton stoichiometry in Tree Top Pond was shaped only weakly by seston food quality, but strongly and consistently by temperature, with

additional contributions from taxa-specific life-history traits. As observed in other systems, the interaction between temperature and taxa appears to be a dominant driver of elemental composition in freshwater zooplankton, suggesting that ongoing climate warming may restructure nutrient cycling dynamics through both physiological and community-level pathways (Bullejos et al., 2014; Moody et al., 2017).

Taken together, these findings suggest that temporal dynamics and warming can alter the elemental balance of dominant freshwater grazers in ways that may influence their growth potential (Villar-Argaiz et al., 2002; Elser et al., 2003), competitive dynamics (Sterner & Elser, 2002; Hessen et al., 2013), and nutritional value up trophic levels (Frost et al., 2005; Hessen & Andersen, 2008; Wagner et al., 2013; Moody et al., 2017). The convergence of %P between *Daphnia* and copepods implies that seasonal warming could erode functional differences between taxa that have traditionally been used to predict community-level stoichiometric patterns. Moreover, declines in %C and %P under increased temperatures may reduce the allocation of lipids and RNA (Prater et al., 2018; Balseiro et al., 2021), with potential consequences for trophic transfer efficiency (Elser et al., 2000). By showing that temperature and seasonal dynamics can outweigh food quality effects for specific taxa, this study highlights the importance of environmental context in shaping zooplankton stoichiometry and identifies a pathway through which climate change may alter freshwater food-web processes.

CHAPTER 2: SPATIOTEMPORAL CHANGES IN SESTON ELEMENTAL COMPOSITION IN A EUTROPHIC, DIMICTIC LAKE

INTRODUCTION

Phytoplankton are the base of aquatic food webs, driving primary production and fueling higher trophic levels (Reynolds, 1984; Wetzel, 2001; Winder & Sommer, 2012). Phosphorus (P) and nitrogen (N) are often limiting nutrients that constrain phytoplankton productivity and biomass (Carpenter et al., 1998; Elser et al., 2007; Schindler et al., 2016; Paerl et al., 2016; Wurtsbaugh et al., 2019). In freshwater ecosystems, phytoplankton communities consist of a wide range of diverse taxa, including, but not limited to, Chlorophyta, Bacillariophyta, Cryptophyta, Dinoflagellata, and Cyanophyta but are often studied collectively as seston, consisting of the suspended matter pool of organic and inorganic particles. However, the composition of seston is highly variable, reflecting both biological activity and inorganic processes. For example, in dimictic lakes, spring and fall mixing can increase sediment content in seston due to resuspending material from the bottom of the lake under mixed conditions (Hilton et al., 1985; Diehl et al., 2002), which can alter the elemental composition of seston. During stratification, a period of increased water column stability, sediment particles will sink, shifting the seston composition to be dominated by biological material, such as phytoplankton and bacterioplankton (Elser et al., 1995; Sterner & Elser, 2002). While we have an understanding of the temporal dynamics of carbon (C), N, and P (Hecky & Kilham, 1988; Sterner, 1989; Wetzel, 2001), we know less about other essential elements.

It is critical to examine the temporal dynamics of elements beyond C, N, and P to gain understanding of how elements are trophically-transferred through aquatic ecosystems in the Anthropocene. The predominant focus on N and P in these systems likely stems from the fact that human activities have significantly altered global nutrient cycles, doubling the amount of biologically available nitrogen (Vitousek et al., 1997; Baron et al., 2013), and tripling the amount of bioavailable phosphorus in global nutrient cycles above pre-industrial levels (Daneshgar et al., 2018). However, anthropogenic influences extend beyond N and P cycles. The bioavailability and concentration of most, if not all, elements in global biogeochemical cycles have rapidly increased over the 20th century (Sen & Peucker-Ehrenbrink, 2012; Tchounwou et al., 2012; Wurtsbaugh et al., 2019; Ochoa-Hueso et al., 2023). For instance, more than 50% of the global cycling of trace-metals such as molybdenum (Mo) (Wong et al., 2021), and manganese (Mn) (Dey et al., 2023) are anthropogenically derived. Additionally, the global biogeochemical cycling of macro-elements, like magnesium (Mg) and potassium (K), has increased by more than 20% compared to pre-industrial levels (Sen & Peucker-Ehrenbrink, 2012). Thus, understanding how non-C, N, and P elements are affected by these changes may reveal how macro-elemental limitations are influencing the micro-elemental composition in lower trophic levels or vise-versa.

While ecological stoichiometry creates the foundation for analyzing the flow of nutrients like C, N, and P through organisms and their environment, the movement of other elements through freshwater ecosystems remains less understood. The ionome represents “the mineral nutrient and trace element composition of an organism and

represents the inorganic component of cellular and organismal systems" (Salt et al., 2008). Ionomics, the study of these elemental linkages, examines how an organism's elemental composition is influenced by environmental stimuli, developmental state, and genetic modifications. The field of ionomics is relatively new and draws from "omics," a multi-discipline category of biological science that investigates the functions and interactions of biological molecules while acknowledging the organism's environmental context (Nguyen et al., 2022). The purpose of ionomics is to provide both qualitative and quantitative insight into an organism's elemental composition (Salt et al., 2008; Jeyasingh et al., 2017), while assessing the relevance of elemental balance shifts to the expression of physiological traits and organismal functioning (Jeyasingh et al., 2020). Much like ecological stoichiometry, ionomics has the power to capture and compare the physiological state of organisms (Salt et al., 2008; Jeyasingh et al., 2017) and can provide insight into supply and elemental demands that can be used to predict ecosystem-wide processes (Jeyasingh et al., 2020).

The crux of ionomics lies in its ability to analyze interactions between elements, regardless of their essentiality (Nguyen et al., 2022). Within complex organisms, a change in the concentration of one element impacts all other elemental balances (Parent et al., 2013). Such alterations to the ionome can result in system-wide elemental proportional changes and provide functional information about an organism, such as growth rate, under different environmental conditions (Salt et al., 2008; Jeyasingh et al., 2017). This was first discovered in plants by Baxter et al. (2008), who found that manipulating soil iron (Fe) levels in *Arabidopsis* resulted in differential uptake of other

elements. Specifically, plants fertilized with Fe exhibited increased uptake of cobalt (Co), zinc (Zn), cadmium (Cd), and Mn (Baxter et al., 2008). Similarly, Watanabe et al. (2015) found that altering N levels in soil resulted in differential uptake of macro and micronutrients in maize. It was found that crops fertilized without N displayed increased assimilation of calcium (Ca), Mg, and K, whereas crops fertilized without P showed higher levels of Mg and K but reduced sodium (Na) (Watanabe et al., 2015). Similarly, wheat seedlings grown in low P conditions resulted in lower concentrations of K, Ca, Na, Mg, Mn, Zn, and silicon (Si), while Fe and sulfur (S) concentrations increased (Chunyan et al., 2022). While these examples illustrate the impacts of environmental nutrient conditions on an organism's ionome, differential nutrient uptake can be a strategy for an organism to maintain homeostasis and cellular processes.

When a required nutrient is limiting, organisms may reduce cellular quotas for that element by modifying their biochemical allocation and composition, such as plankton producing non-P lipids in order to use available P for non-membrane needs (Van Mooy et al., 2009; Bellinger et al., 2014; Jeyasingh et al., 2023). Similarly, organisms can increase their uptake of specific nutrients to compensate for deficiencies and maintain cellular functions. For example, when in P-limited environments, some plants have been observed to increase Zn uptake to prevent formation of P-required complexes (Misson et al., 2005) and to synthesize the P-scavenging enzyme, alkaline phosphatase (McCarthy et al., 2010; Wagner & Frost, 2012; Wang et al., 2022). Such studies have pioneered the use of ionomics as a mechanistic framework for correlating elemental supply stoichiometry, biomolecular allocation, and physiology.

In aquatic systems, environmental variability shapes phytoplankton elemental composition, linking abiotic factors to the seston ionome. Light availability alters pigment requirements, with low-light conditions increasing chlorophyll *a* content relative to C, which in turn increases cellular Mg and N quotas, while high light availability reduces pigment demand (Laws & Bannister, 1980; Geider, 1987; Falkowski & Raven, 2007). These changes can extend to energy metabolism, since Mg associates with phosphate in biomolecules that have a free phosphate group, such as ATP (Pohland & Schneider, 2019; Wagner et al., 2025). Temperature further alters elemental demand, such as cold conditions promoting higher P content through greater ribosome allocation (Yvon-Durocher et al., 2015; Hessen et al., 2017), while warming generally increases C:P and N:P ratios in phytoplankton (Hessen et al., 2005; Yvon-Durocher et al., 2015).

Community composition contributes more variability. For example, dominance by organisms within the Bacillariophyta phyla can increase Si content in seston (Sommer et al., 1986; Conley et al., 1989), while taxa with high requirements for Fe or K would alter the cycling of trace elements through differences in photosynthetic pigments and enzyme allocation (Sterner & Elser, 2002; Glass et al., 2010). Depending on the community composition, elements used to balance charges across the thylakoid membrane may alter the sestons ionome as well, such as cyanobacteria using K to assist in generating the proton gradient (Checchetto et al., 2013). Lastly, in N-limited lakes, the community can shift to be dominated by diazotrophs that have a higher Fe and Mo demand caused by the increased synthesis of nitrogenase, the enzyme responsible for converting atmospheric N_2 into bioavailable ammonia (Glass et al., 2010; Raven, 2012; Wagner et al., 2025). While

several studies have characterized phytoplankton elemental composition in marine systems (Ho et al., 2003; Quigg et al., 2003), little research has examined these patterns in freshwater environments.

AIMS

Here, we investigate how does the seston ionome vary across seasonal environmental gradients? We hypothesize that (1) temporal dynamics will affect seston elemental content due to vertical gradients in physical and chemical lake processes, such as stratification, anoxia, and the associated redox changes with anoxia (e.g. sediment nutrient flux; Sommer et al., 1986; Schindler et al., 1996; Diehl et al., 2002; Winder & Sommer, 2012). We predict that seston elemental content will shift seasonally, with spring mixing homogenizing nutrients throughout the water column, leading to higher proportion of elements associated with sediment, then switching to more biological elements as the seasons progress from spring to fall. We are predicting a seasonal change in phytoplankton succession as described by the Plankton Ecology Group (PEG) model (Sommer et al., 1986). Therefore, we predict that spring should have higher proportions of Si caused by a Bacillariophyta bloom (Reynolds, 2009), then shifting to cyanobacteria dominance in late summer, which may increase the proportion of Fe and K in surface waters (Wagner et al., 2025). In the anoxic hypolimnion, we predict the seston ionome to have higher proportions of Fe, Mn, P, and S that are redox-sensitive (directly or indirectly) and can be found in high concentrations in sediment (Davison, 1993; Hamilton-Tayler & Davison, 1995). Additionally, we hypothesize that (2) temperature will influence seston elemental composition due to its effects on cellular physiology and

metabolism (Sterner & Elser, 2002; Beardall et al., 2009; Winder & Sommer, 2012; De Senerpont Domis et al., 2014; Yvon-Durocher et al., 2015). We predict that seston elemental composition will be moderated by temperature, with warmer conditions increasing the proportion of elements associated with metabolic processes (e.g. P, N, Mg, Fe, and other trace metals required for enzymatic function) (Hamilton-Tayler & Davison, 1995; Somero, 2004).

METHODS

Study site: Seven Ponds Nature Center – Tree Top Pond

We collected seston samples from Tree Top Pond located within Seven Ponds Nature Center in Dryden, MI (USA). Tree Top Pond is a temperate, eutrophic, dimictic lake reaching a max depth of 11m, with a surface area of 15,161.56 m^2, and a total volume of 24,258m^3 (24,258,000L). The surrounding area is dominated by forested land (45.61%), woody wetlands (19.43%), pasture (15.38%), agricultural crop land (7.17%), and developed area (5.68%) (Stroud Water Research Center, 2017).

Field sampling

Weekly sampling was conducted from March through September 2024, a period that comprised both the typical growing season and the course of seasonal plankton succession pattern in northern temperate lakes (Sommer et al., 1986; Prater et al., 2018). At the deepest point of the lake, we collected water to analyze particulate matter concentrations. Shortly after ice-off, we collected samples from the surface, 5m, and 9m using a Van Dorn during holomixis conditions. Once stratification developed, we began

to collect samples at every meter from the surface to 9m. Water was stored on ice in acid-washed 2L bottles and returned to the lab for processing.

In addition, a buoy was deployed at the center of Tree Top Pond with eight HOBO sensors (Onset), positioned between the surface and 9.3m. These sensors recorded temperature and dissolved oxygen every 15 minutes. Dissolved oxygen sensors were recalibrated monthly, and all sensors were checked regularly for fouling. The buoy data provided continuous information on water column temperature and oxygen.

Seston particulate C, N, and P analysis

Filters for particulate P concentrations were transferred to glass vials and digested in a hot 1.65% potassium persulfate solution following established protocols (Wagner & Frost, 2012; Prater et al., 2018). P concentrations were then analyzed via molybdate-blue ascorbic acid colorimetry, with absorbance measured spectrophotometrically using either a 1 or 5cm cuvette, depending on the expected concentration (APHA, 1992). Particulate filters for CN were oven-dried at 60°C for 24h and subsequently analyzed using a Costech 4010 elemental analyzer, following Wagner & Frost (2012).

Sample processing

Particulate samples for ionomic analysis were filtered onto cellulose acetate 0.45µm filters for each depth (0-9m). Filters were labeled and stored at -20°C until processing. They were then dried at 60°C and shipped to the University of Arkansas. To prep the samples for analysis, they were extracted in 15mL polypropylene tubes for 3 days, using 600µL of a 2:1 (v/v) solution of 70% trace clean nitric acid and hydrogen

peroxide solution. After extraction, the samples were diluted to 6.5mL with MilliQ water and analyzed on an inductively coupled plasma optical emission (ICP-OES) 230 spectrometer (ICP, Thermo Scientific iCAP 7400). To correct for potential matrix effects, samples were run with an in-line internal standard of yttrium (CPI International, Santa Rosa, CA), and digestion efficiencies were estimated using a multi-elemental muscle tissue standard (CPI International, Santa Rosa, CA) and used to correct sample elemental composition measurements. Calibration of the ICP-OES used an external calibration standard reference solution (CPI International, Santa Rosa, CA).

Statistical analysis

Prior to analysis, we applied a centered log-ratio (CLR) transformation to the concentration data of each element using the compositions package in R (van den Boogaart & Tolosana-Delgado, 2008). This transformation comes from compositional data analysis, which allows for analysis of variables that represent parts of a whole. CLR transformations show each component as the natural logarithm of its ratio to the geometric mean of the whole composition (Aitchison, 1982, 1986). The CLR transformation takes the seston compositional data and presents each element relative to the others, removing the influence of concentration differences and expressing the proportional relationship between elements.

To evaluate hypothesis 1, that states that temporal dynamics will affect seston elemental content due to vertical gradients in physical and chemical lake processes, we conducted a principle component analysis (PCA) using the CLR-transformed data using the prcomp() function in R. The CLR transformation allows for the pairwise comparison

of all elements in multivariate space (Greenacre et al., 2021). In the PCA ordinations, element vectors pointing in the same or opposite direction suggest coupled responses, while orthogonal vectors indicate no correlation between elements. We plotted the data by month to observe any temporal trends in elemental composition.

Additionally, we conducted a two-way multivariate analysis of variance (MANOVA) on the CLR-transformed composition of each element individually to examine how the ionome changed by month, depth, and their interaction. We used Pillai's trace to approximate F-values, using the car package (Fox et al., 2024) with MVN (Korkmaz et al., 2014), biotools (Silva et al., 2017), and base R functions to check model assumptions of multivariate normality (Mardia's, Henze-Zirkler's, and Royston's tests), homogeneity of covariance (Box's M test), and collinearity (cor()). As we found the whole ionome had significant interactions between month and depth, we then performed a two-way analysis of variance (ANOVA) using the Anova() function from the car package for each element (Fox et al., 2024).

To evaluate hypothesis 2, that temperature alters seston elemental content, we used linear regression. We used the average temperature at each depth as the independent variable, and the CLR-transformed concentrations of each element at each depth were used as the dependent variable. Data points were colored by depth to visualize patterns. A significant relationship would suggest that temperature is a driver of the element concentration within the seston, regardless of depth.

RESULTS

We examined how the seston elemental concentrations varied spatiotemporally (Fig 2.1 & Fig. 2.2). Aluminum (Al) concentration was generally stable (~0.5-2 µg/L) in the seston, except for elevated concentrations in early April (25.5 µg/L; Fig 2.1). Seston barium (Ba) remained <2 µg/L throughout most of the sampling period, with the exception of a mid-depth spike in late September. Carbon was initially low in the seston (<500 µg/L) until May, after which concentrations rose to 700-1000 µg/L throughout the water column, peaking at ~5761 µg/L in August at ~4m (Fig 2.1). Seston calcium (Ca) was highly variable (~45-520 µg/L), with two distinctive peaks in the upper 4m in mid-April and late-June. Calcium accumulated in the anoxic hypolimnion from late-July through September, reaching concentrations as high as ~520 µg/L. Chromium (Cr) was consistently low (~0.08-0.78 µg/L), with early season variability across depths, followed by declines after April. In late July, concentrations spiked at 1m and then declined, while Cr began to accumulate in bottom sediments through the end of the season. Iron (Fe) fluctuated in seston between ~25 and ~50 µg/L in the upper 5m until late-August, when it decreased to ~9 µg/L. However, Fe concentrations in the hypolimnion steadily increased, reaching a maximum of ~965 µg/L by the end of September. Seston potassium (K) was stable (<6 µg/L) for much of the season but increased to 10-17 µg/L in September between 4 and 9m. Magnesium (Mg) was relatively uniform in the seston (~10-15 µg/L) until late June, when concentrations rose (~25 µg/L), followed by an increase at 9m in late July (~60 µg/L) that persisted through the end of the season (Fig 2.1).

Seston manganese (Mn) concentration ranged widely, from ~4 µg/L to ~165 µg/L, with early spring values of ~20-35 µg/L across depths (Fig 2.2). After declining in April, Mn became concentrated between 5-7m, where it reached a seasonal maximum (~165 µg/L). Nitrogen concentration remained stable in March-April (~60 µg/L) in the seston before increasing from 5-9m in May (~200 µg/L) and expanding upward to 3m in late July, peaking at ~930 µg/L in early September at 4m. Seston sodium (Na) was relatively stable, between 1 and 10 µg/L, throughout the water column, though we observed spikes in mid-May (~30 µg/L) and July (~20 µg/L) in the top 2m. Phosphorus (P) concentrations were consistently low (<10 µg/L) in the seston until May, then increased below 4m through September, reaching a maximum of ~67 µg/L at 9m. Sulfur (S) content was below 30 µg/L until June, then peaked in surface layers in July; S concentration increased from late-July through September, from 4 to 6m, to 30 µg/L and accumulated to ~190 µg/L at 9m. Silicon (Si) concentration in seston was above 30 µg/L throughout the water column until September when content decreased. We observed two periods of higher concentrations, one occurring from March to April and in July, reaching a maximum ~90 µg/L. Seston Strontium (Sr) concentrations remained uniform (~0-0.4 µg/L) except for late-season increases at mid and bottom depths. Finally, Zinc (Zn) content was generally low in the seston (<1 µg/L), with short-lived spikes (~5 µg/L) at multiple depths in April and May.

We examined the temporal trends in the seston ionome using PCA (Figure 2.3, 2.4, & 2.5). The elemental trends across depth generally followed a similar temporal pattern. At most depths, the proportion of Al and Mn in seston was higher in March and

April (Fig 2.3, Fig 2.4, & Fig 2.6). In May, the proportion of Si within the seston increased at all depths. At most depths, the proportion of P and Mg was higher in the seston in June. Finally, by September, the proportion of Ca and K increased in the seston (Fig 2.3, Fig 2.4, & 2.5).

In the surface waters (0-3m; Fig 2.3), seston in March and April had a greater proportion of Al, Fe, and Mn, and a lower proportion of N, C, Mg, S, and Ca, patterns largely explained by axis 1. In May and June, we found a greater proportion of Si and P, primarily explained by axis 2. From July to September, we found greater proportions of N, C, Mg, S, and Ca in the seston, with corresponding declines in Al, Fe, and Mn. At these depths, the first two principle components accounted for 62.4% at 0m, 57.1% at 1m, 61.0% at 2m, and 62.6% at 3m of the variation explained.

Mid-depth samples (4-6m; Fig 2.4) had a greater proportion of Al, Fe, Mn, and Si in April and May, with less S, C, N, P, and K, explained by axis 1. In June, there were greater proportions of Mg and Ca at 4 and 5m, which was largely explained by axis 2, while at 6m, axis 2 was instead driven by a lower Zn in May and June. From August to September, seston at 4 and 5m had higher proportion of C, N, P, and K, which was explained mostly by axis 1, whereas seston at 6m showed a distinct increase in Mg by September. The first two principle components explained 58.0% at 4m, 62.8% at 5m, and 59.0% at 6m of the total variation.

We found clear distinction in the temporal patterns between 7 and 8m depth, and 9m (Fig 2.5). At 7 and 8m, there was a higher proportion of Al, Mn, and Fe in April and May, with Al and Mn being explained by axis 1 and Fe by axis 2 at 8m. By July, the

seston at these depths had a higher proportion of Mg, S, C, N, and P, shifting to Ca and K in September. At 9m, the proportion of Al and Mn were high from March to May, followed by increased C, N, P, Si, and Mg in May and June, mostly explained by axis 2. In July, the seston had higher Fe and S, which was explained by axis 1, and by September, seston had higher proportions of Ca, Sr, and Ba. Despite these differences, the proportion of variation explained by the first two principle components were consistent across depth, with 59.5% at 7m, 61.0% at 8m, and 61.5% at 9m.

To examine how the ionome varied by month and depth, we performed a MANOVA that indicated whether month significantly interacted with depth (Table 2.1). To further understand the influence of the ionome temporally and by depth, we analyzed the individual elements by month and depth using a univariate two-way ANOVA (Table 2.2). Month significantly influenced all CLR-transformed elements except Cr, while depth was found to be a significant factor for every element. The interaction between month and depth was also significant for most elements, with the exceptions of Al, Ca, Cr, and Zn.

We found temperature affected many of the seston elemental contents (Fig 2.6; Table 2.3). The proportion of Al, Ba, Fe, and Mn negatively correlated with temperature. In contrast, the proportion of C, Ca, K, N, Na, S, Sr, and Zn positively correlated with temperature. In all instances, deeper depths remained cold throughout the year while shallower depths warmed in the spring and summer.

Table 2.1. Multivariate analysis of variance (MANOVA) results for the effect of month and depth on seston ionome. Represented is the F-value, p-value, and Pillai's trace for each factor.

MANOVA			
Factor	**F-value**	**p-value**	**Pillai**
Month	14.9245	**<0.001**	2.7923
Depth	5.5233	**<0.001**	2.8260
Month x Depth	2.2223	**<0.001**	6.2266

Table 2.2. Analysis of variance (ANOVA) results for each seston ionome element, exploring the effects of month, depth, and their interaction (month x depth). For each element, the table shows the F-value, p-value, and percent of variance explained by each factor.

ANOVA				
Element (centered log transformed)	**Factor**	**F-value**	**p-value**	**Percent of variance explained**
Al	Month	96.53	**<0.001**	80.84
	Depth	9.15	**<0.001**	13.79
	Month x Depth	0.51	0.99	3.86
Ba	Month	16.04	**<0.001**	9.58
	Depth	28.31	**<0.001**	30.41
	Month x Depth	7.02	**<0.001**	37.69
C	Month	46.13	**<0.001**	38.27
	Depth	10.62	**<0.001**	15.86
	Month x Depth	1.99	**<0.001**	14.85
Ca	Month	18.24	**<0.001**	19.07
	Depth	16.65	**<0.001**	31.32
	Month x Depth	1.12	0.30	10.53
Cr	Month	1.64	0.15	3.16
	Depth	2.53	**0.009**	8.78
	Month x Depth	0.91	0.63	15.85
Fe	Month	25.40	**<0.001**	9.03
	Depth	90.12	**<0.001**	57.65
	Month x Depth	6.26	**<0.001**	20.03
K	Month	38.65	**<0.001**	39.31
	Depth	4.03	**<0.001**	7.37
	Month x Depth	1.67	**0.009**	15.27
Mg	Month	65.44	**<0.001**	43.42
	Depth	14.14	**<0.001**	16.89
	Month x Depth	2.49	**<0.001**	14.87
Mn	Month	49.70	**<0.001**	26.68
	Depth	21.41	**<0.001**	20.70
	Month x Depth	6.73	**<0.001**	32.54
N	Month	37.77	**<0.001**	30.83
	Depth	15.92	**<0.001**	23.39
	Month x Depth	2.08	**<0.001**	15.26

Table 2.2. Continued.

ANOVA				
Element (centered log transformed)	**Factor**	**F-value**	**p-value**	**Percent of variance explained**
Na	Month	34.45	**<0.001**	32.49
	Depth	11.38	**<0.001**	19.31
	Month x Depth	1.52	**0.027**	12.93
P	Month	13.32	**<0.001**	8.81
	Depth	37.28	**<0.001**	44.36
	Month x Depth	3.72	**<0.001**	22.11
S	Month	103.89	**<0.001**	50.21
	Depth	15.68	**<0.001**	2.74
	Month x Depth	4.16	**<0.001**	3.63
Si	Month	47.04	**<0.001**	34.92
	Depth	3.69	**<0.001**	4.94
	Month x Depth	1.68	**0.009**	11.22
Sr	Month	26.50	**<0.001**	23.90
	Depth	13.17	**<0.001**	21.37
	Month x Depth	2.59	**<0.001**	21.01
Zn	Month	9.01	**<0.001**	16.02
	Depth	2.30	**0.017**	7.38
	Month x Depth	0.63	0.97	10.09

Table 2.3. Summary of linear regression analyses examining the correlation between individual sestion ionome elements and temperature. The regression equation, degree of freedom (df), adjusted r^2, F-value, and p-value are shown for each element, with degree of freedom written as numerator, denominator. Significant regressions (<0.05) are shown in bold.

Element	Regression equation	df	r^2	F-value	p-value
Al	y = 0.026x + 2.32	1, 254	0.36	144.1	**<0.001**
Ba	y = 0.007x – 3.43	1, 254	0.014	4.58	**0.033**
C	y = 0.02x + 4.28	1, 254	0.108	31.95	**<0.001**
Ca	y = -0.05x + 2.31	1, 254	0.29	107.3	**<0.001**
Cr	y = 0.006x -1.23	1, 254	<0.001	0.81	0.37
Fe	y = 0.013x + 0.50	1, 254	0.18	57.22	**<0.001**
K	y = -0.02x + 1.09	1, 254	0.064	18.49	**<0.001**
Mg	y = 0.002x + 2.67	1, 254	-0.002	0.36	0.55
Mn	y = 0.015x – 0.55	1, 254	0.099	29.1	**<0.001**
N	y = -0.0176x – 2.04	1, 254	0.069	19.93	**<0.001**
Na	y = -0.029x + 0.64	1, 254	0.19	62.15	**<0.001**
P	y = -0.0087x – 1.36	1, 254	0.002	1.62	0.20
S	y = 0.013x + 0.82	1, 254	0.094	27.62	**<0.001**
Si	y = 0.006x + 1.29	1, 254	<0.001	1.21	0.27
Sr	y = 0.006x – 4.02	1, 254	0.022	6.64	**0.011**
Zn	y = 0.015x – 3.29	1, 254	0.016	5.26	**0.023**

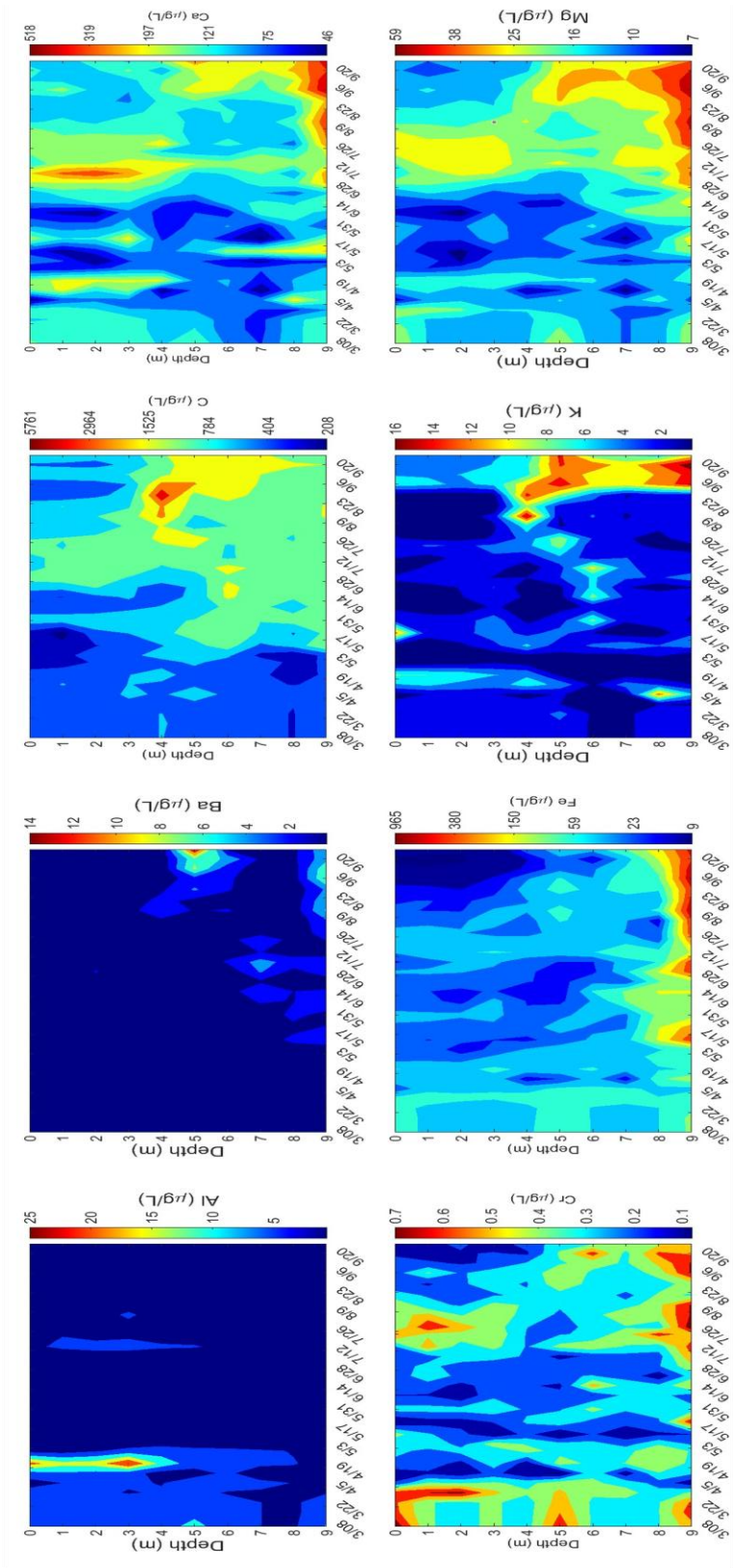

Figure 2.1. Depth-time contour plots of seston aluminum (Al), barium (Ba), carbon (C), calcium (Ca), chromium (Cr), iron (Fe), potassium (K), and magnesium (Mg) concentrations from March to September 2024. Each panel shows the vertical distribution of a single element (µg/L), with warmer colors indicating higher concentrations and cooler colors lower concentrations, with the depth (m) axis inverted. Concentrations above 30 µg/L are displayed on a log scale. Color scales are element-specific to reflect differences in concentration range.

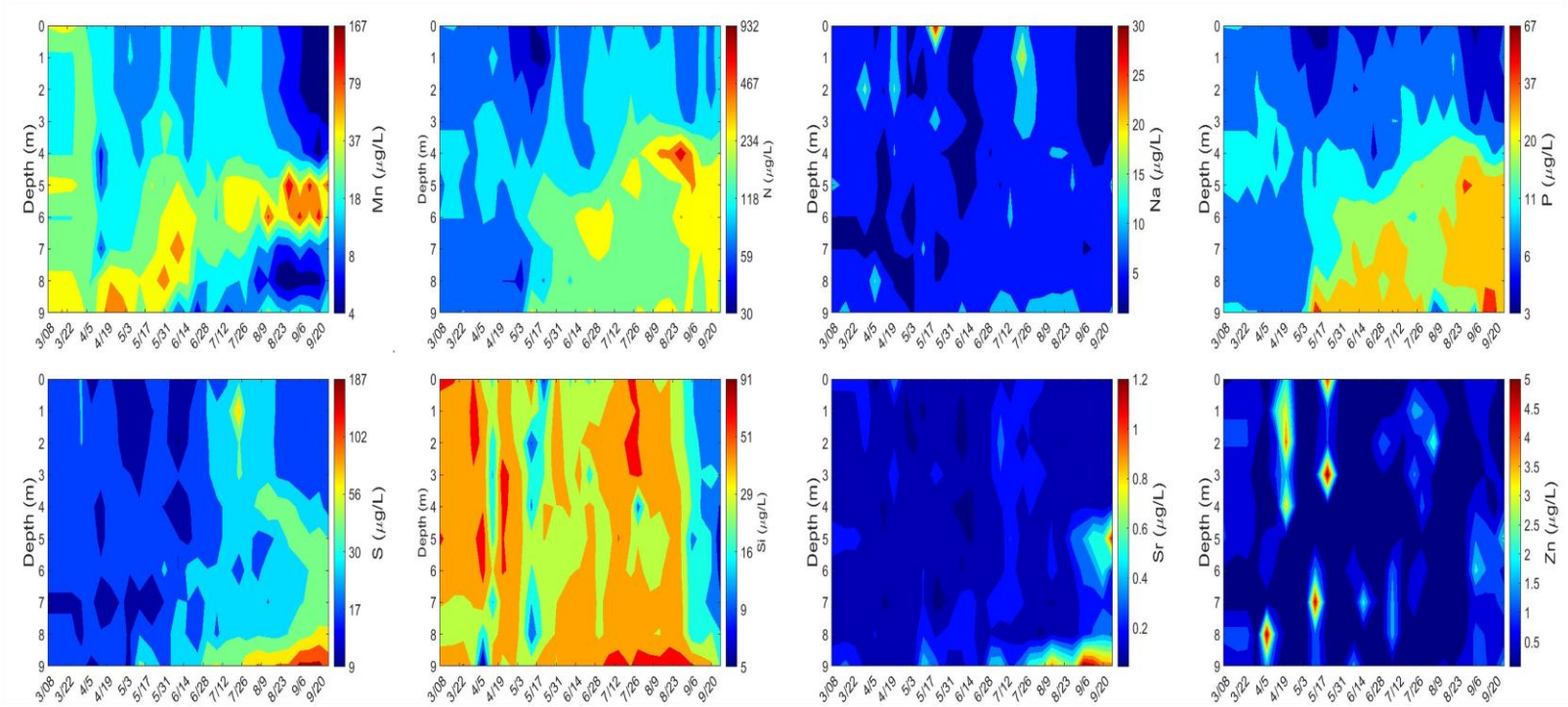

Figure 2.2. Contour plots showing the temporal and vertical patterns of seston manganese (Mn), nitrogen (N), sodium (Na), phosphorus (P), sulfur (S), silicon (Si), strontium (Sr), and zinc (Zn) concentrations from March to September 2024. Each panel shows the concentration of a single element (µg/L), with warm colors indicating higher abundance and cooler colors showing lower concentrations, and depth (m) inversed. A log scale was used for concentrations above 30 µg/L.

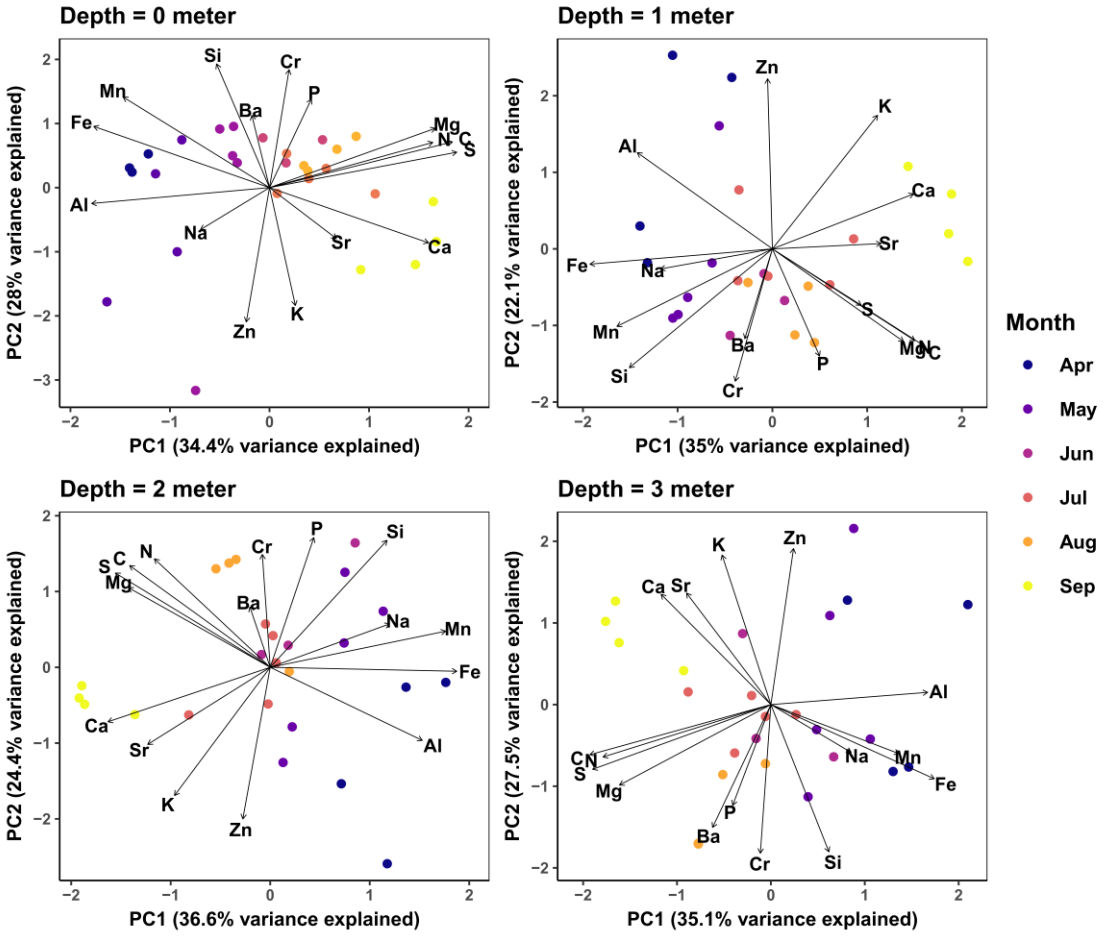

Figure 2.3. Principle component analysis (PCA) of seston ionome for 0-4m depth. Each point represents a single sample plotted according to its scores on the first two principle components (PC1 and PC2), which together explain the total variance in elemental composition. Elements contributing most to the principle component are shown as vectors, indicating direction and strength of their influence on the samples. Color of data point designates the month in which samples were collected (March-September 2024); cooler colors show earlier samples and warmer colors indicate later samples.

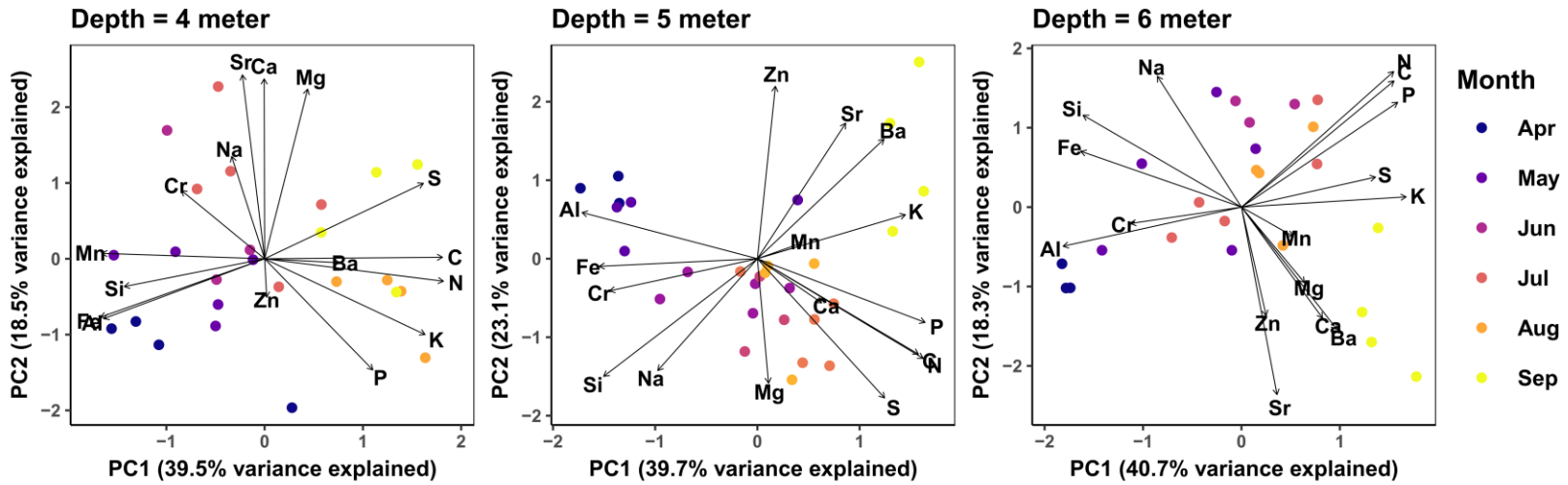

Figure 2.4. Principle component analysis (PCA) of seston ionome across 4-6m depth. Datapoints show a single sample plotted based on its scores across the first two principle components (PC1 and PC2) and together explain the total amount of variance in seston composition. Elements are shown as arrows, indicating the strength and direction of their influence on the elemental composition. Color of data point indicates the month in which the sample was collected, starting in March and ending in September 2024; cooler colors indicate earlier sampling months, and warmer colors represent later samples.

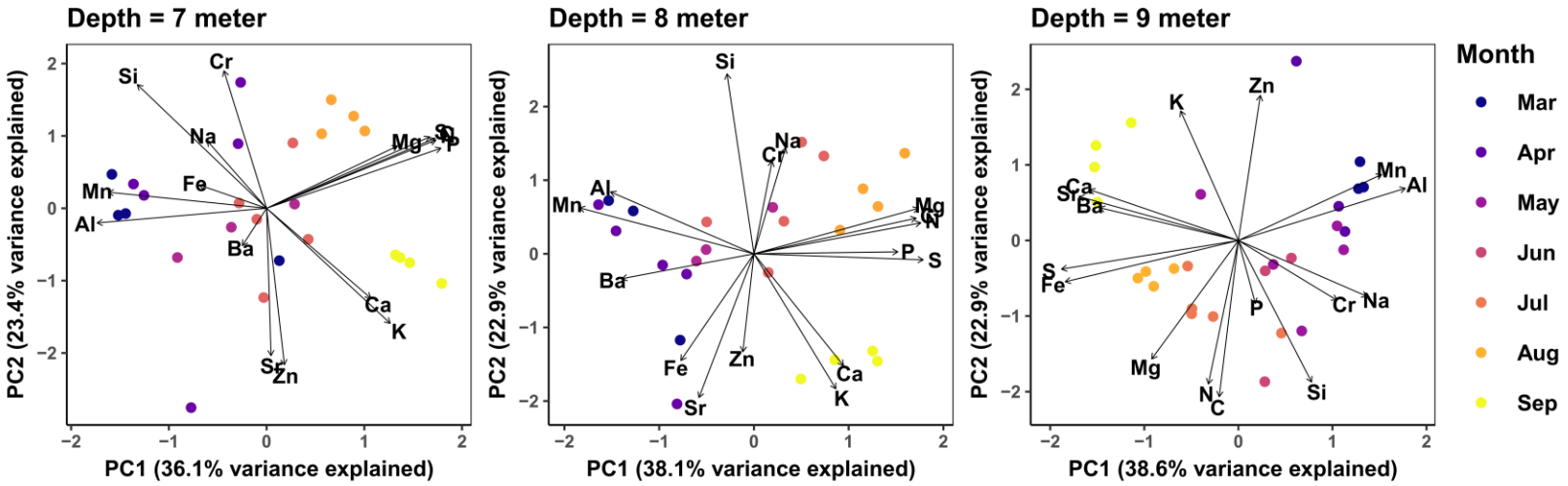

Figure 2.5. Principle component analysis (PCA) of seston ionome across 7-9m depth. Datapoints show a single sample plotted based on its scores across the first two principle components (PC1 and PC2) and together explain the total amount of variance in seston composition. Elements are shown as arrows, indicating the strength and direction of their influence on the elemental composition. Color of data point indicates the month in which the sample was collected, starting in March and ending in September 2024; cooler colors indicate earlier sampling months, and warmer colors represent later samples.

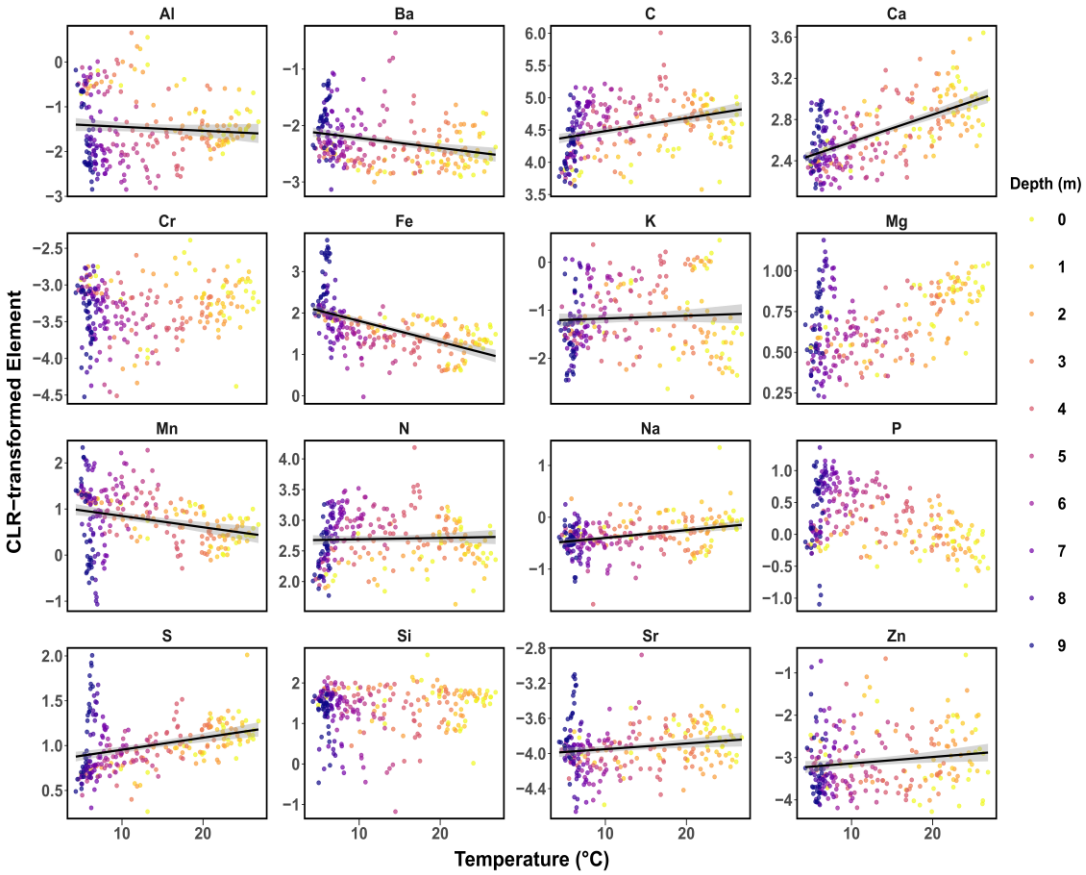

Fig 2.6. Linear regressions of CLR-transformed seston elements against temperature (°C). Each point is colored by the depth of the sample, with warmer colors for surface depths and cooler colors for deeper samples. Regression lines are shown only for significant relationships, with 95% confidence intervals shown in grey shading.

DISCUSSION

We found that the elemental composition of seston in Tree Top Pond was driven by spatiotemporal dynamics, with month and depth-dependent influences on elemental composition. Seston elemental composition varied across depth, reflecting vertical gradients of physical and chemical processes (Schindler et al., 1996; Diehl et al., 2002; Winder & Sommer, 2012). These results provide partial support for hypothesis 1, that temporal dynamics alter seston elemental content through vertical gradients of lake processes. Specifically, we saw higher Si proportions in the early spring, as predicted by the PEG model (Reynolds, 2009; Sommer et al., 1986). However, we did not find evidence of increased elements associated with cyanobacteria (Fe and K). Additionally, we saw greater proportion of redox-sensitive elements, such as Fe and Mn, as well as sediment-associated elements like Al, throughout the water column under mixed conditions but the proportion of these elements declined as the season progressed (except for Fe at 9m). We also found support for hypothesis 2, that temperature would influence seston elemental composition, but our data did not support our predictions. Elements associated with metabolic processes, such as Mg and P, had no relationship with temperature, N had little influence, and Fe was negatively affected. Despite contradicting our predictions, almost all other elements had a significant relationship with temperature, though the directionality of the proportional changes were element-dependent, reinforcing the role of seasonal warming in altering elemental dynamics.

Sediment is resuspended during mixing conditions occurs shortly after ice-off, when the entire water column becomes isothermal and wind energy can reach the bottom

of the lake (Wetzel, 2001). Previous studies have found sedimentation rates are highest during mixing conditions during spring and fall overturns (Hilton, 1985; Filstrup & Lind, 2010), that likely account for sediment being picked up in the littoral regions and transported via advection to the pelagic zone. The elemental composition of sediments can be highly variable, depending on both lake geology and trophic status (Søndergaard et al., 2003). Many lake sediments contain clay (Al and Si; Stumm & Morgan, 1996), and redox-sensitive metals such as Mn and Fe often undergo geochemical focusing. Under oxic conditions, these elements precipitate as oxides and hydroxides near the sediment-water interface (Scholtysik et al., 2022; Davison, 1993). Consistent with these processes, we observed higher proportions of Al, Mn, and Fe throughout the water column (except Fe at 9m) shortly after ice-off, likely reflecting sediment resuspension and redistribution during spring mixing. As stratification developed, these particles settled, and the proportion of Al, Mn, and Fe in seston decreased.

The elemental composition of seston reflects the temporal characteristics of northern temperate lakes. According to the PEG model, phytoplankton communities transition from Bacillariophyta dominance in the spring to green algae and cyanobacteria in the summer (Sommer et al., 1986; Adrian et al., 1999, 2006). Following ice-off, low temperatures, weakened stratification, and limited light constrain phytoplankton growth, resulting in low chlorophyll *a* concentrations, a proxy for biomass (Sommer et al., 1986; Smol, 1988). As surface waters warm and stabilize, nutrient-rich conditions and increased light stimulate the first phytoplankton blooms of the year, typically dominated by diatoms (Sommer et al. 1986; Adrian et al., 1999, 2006). The timing and magnitude of this spring

bloom is strongly influenced by winter ice cover (Hampton et al., 2015, Warner et al., 2018), air temperature (Adrain et al., 1999, 2006; Rühland et al., 2008), and nutrient availability (Hampton et al. 2015; Smol, 1988). Because Bacillariophyta has frustules made of Si, the proliferation of this taxon increases the proportion of Si in suspended particulates (Ragueneau et al., 2000; Reynolds, 1984, 2009). Accordingly, the high proportion of Si in seston from the surface in May and June likely corresponds to a Bacillariophyta dominated spring bloom.

Interestingly, from June to August, increased seston P concentrations were associated with higher Mg proportions across most depths. In lakes, P can be associated with different material pools: absorbed to clay, bound to Fe and Al oxides, or incorporated into organic matter (Wetzel, 2001; Søndergaard et al., 2003). In organisms, P is an essential component for phospholipids, nucleic acids, energy molecules (i.e., ATP), and cellular signaling pathways (Elser et al. 1996; Sterner and Elser 2002; Hessen et al. 2013; Wagner et al. 2013). Because phosphate groups are negatively charged, they are often stabilized by association with Mg ions (Schneider & Kabeláč, 1998). Although Mg can be absorbed to clay particles (Mackereth, 1997), the lack of relationship between Al and Mg in our data suggests that the higher proportion of Mg and P in the seston was primarily biologically derived.

Later in the season, the proportions of Ca, Ba, and Sr increased across most depths during September, except at 4 and 5m. These elements share similar geochemical behavior because they belong to the alkaline earth metal group and often co-precipitate with carbonate minerals (Stumm & Morgan, 1996). Calcite ($CaCO_3$) precipitation (i.e.,

calcium carbonate) is common in low salinity temperate lakes and can be induced by temperature, pH, and wind driven mixing of the epilimnion (Stabel, 1986). High phytoplankton productivity, particularly by cyanobacteria and picoplankton, can increase pH levels through CO_2 uptake, promoting carbonate precipitation involving Ca and Sr (Otsuki & Wetzel, 1972; Hodell et al., 2003; Dittrich & Obst, 2004). The lack of a direct correlation between C and Ca, Sr, or Br likely reflects the role of C in both organic biomass and inorganic carbonate precipitation. This may explain why in our PCA, C correlated with N and S, more than Ca and Sr, indicating that most particulate C was organically derived rather than carbonate associated.

Temperature was strongly correlated with many elements. In our strongly stratified lake, however, it is difficult to disentangle direct temperature responses from depth effects because they are highly correlated (e.g., colder water at the bottom). We predicted higher proportions of elements associated with metabolic processes; however, we instead observed increases in elements typically elevated in phytoplankton (C, N, S; Sterner & Elser, 2002) with rising temperature, representing a biological trend likely driven by increased phytoplankton densities. Alternatively, we found that elements associated with geochemistry and biology, such as Fe, Ca, and Sr, had conflicting relationships depending on whether they were concentrated near the surface or bottom waters. The positive association of Ca and Sr with temperature may reflect increased carbonate precipitation during high chlorophyll *a* periods (Dittrich & Obst, 2004). Conversely, Fe showed a negative relationship with temperature, potentially due to redox-driven precipitation during sample handling. In the anoxic hypolimnion, the

dominate form of Fe is soluble (Fe II), but when exposed to oxygen during transport and filtering, it oxidizes to Fe III (Wetzel, 2001), forming insoluble hydroxides that precipitate out (Davison, 1993). This oxidation could explain the negative relationship of Fe content in seston from colder, anoxic waters.

Overall, the seston ionome was influenced by geochemical and biogeochemical processes. During spring mixing, the seston composition reflected strong geochemical and biogeochemical signatures linked to sediment resuspension and carbonate precipitation, respectively. However, during late spring and summer, microbial communities dictated the ionomic profile, dominated by macronutrients in plankton. The timing and extent of this transition are likely lake-specific, influenced by lake morphology, geology, and mixing regime (Wetzel, 2001; Håkanson, 2005). Depending on the timing and onset of summer stratification, the temporal variation in the ionome will likely be dynamic. The onset of stratification separates the epilimnion and hypolimnion N and P concentrations that are known to shape phytoplankton communities (Watson et al., 1997; Winder & Sommer, 2012), which may influence the ionome composition. Future studies should extend ionomic monitoring across multiple years and trophic gradients to determine whether the observed seasonal transitions are consistent across ecosystems.

LITERATURE CITED

Acharya, K., M. Kyle, and J. J. Elser. 2004. Biological stoichiometry of *Daphnia* growth: An ecophysiological test of the growth rate hypothesis. Limnology and Oceanography **49**: 656–665. doi:10.4319/lo.2004.49.3.0656

Adrian, R., N. Walz, T. Hintze, S. Hoeg, and R. Rusche. 1999. Effects of ice duration on plankton succession during spring in a shallow polymictic lake. Freshwater Biology **41**: 621–634. doi:10.1046/j.1365-2427.1999.00411.x

Adrian, R., S. Wilhelm, and D. Gerten. 2006. Life-history traits of lake plankton species may govern their phenological response to climate warming. Global Change Biology 12: 652–661. doi:10.1111/j.1365-2486.2006.01125.x

Aitchison, J. 1982. The statistical analysis of compositional data. Journal of the Royal Statistical Society: Series B (Methodological) **44**: 139–177. doi:10.1111/j.2517-6161.1982.tb01195.x

Aitchison, J.1986. The statistical analysis of compositional data. Journal of the Royal Statistical Society **44**: 416. doi: 10.1111/j.2517-6161.1982.tb01195.x

Allan, J. D. 1976. Life history patterns in zooplankton. The American Naturalist **110**: 165–180.

Andersen, T., and D. O. Hessen. 1991. Carbon, nitrogen, and phosphorus content of freshwater zooplankton. Limnology & Oceanography **36**: 807–814. doi:10.4319/lo.1991.36.4.0807

APHA. 1992. APHA method 4500-P: Standard methods for the examination of water and wastewater, 18th ed. A. E. Greenberg, L. S. Clesceri, and A. D. Eaton [eds.], American Public Health Association.

Arar, E.J. & Collins, G.B. (1997). Method 445.0: Chlorophyll a. U.S. Environmental Protection Agency, **1.2**, 1–22.

Balseiro, E., C. Laspoumaderes, F. Smufer, L. Wolinski, and B. Modenutti. 2021. Short term fluctuating temperature alleviates *Daphnia* stoichiometric constraints. Scientific Reports **11**: 12383. doi:10.1038/s41598-021-91959-w

Baron, J. S., E. K. Hall, B. T. Nolan, J. C. Finlay, E. S. Bernhardt, J. A. Harrison, F. Chan, and E. W. Boyer. 2013. The interactive effects of excess reactive nitrogen and climate change on aquatic ecosystems and water resources of the United States. Biogeochemistry **114**: 71–92. doi:10.1007/s10533-012-9788-y

Barth-Jensen, C., M. Daase, M. R. Ormańczyk, Ø. Varpe, S. Kwaśniewski, and C. Svensen. 2022. High abundances of small copepods early developmental stages and nauplii strengthen the perception of a non-dormant Arctic winter. Polar Biology **45**: 675–690. doi:10.1007/s00300-022-03025-4

Baxter, I. R., O. Vitek, B. Lahner, B. Muthukumar, M. Borghi, J. Morrissey, M. L. Guerinot, and D. E. Salt. 2008. The leaf ionome as a multivariable system to detect a plant's physiological status. Proceedings of the National Academy of Sciences **105**: 12081–12086. doi:10.1073/pnas.0804175105

Beardall, J., S. Stojkovic, and S. Larsen. 2009. Living in a high CO2 world: impacts of global climate change on marine phytoplankton. Plant Ecology & Diversity **2**: 191–205. doi:10.1080/17550870903271363

Becker, C., H. Feuchtmayr, D. Brepohl, B. Santer, and M. Boersma. 2004. Differential impacts of copepods and cladocerans on lake seston, and resulting effects on zooplankton growth. Hydrobiologia **526**: 197–207. doi:10.1023/B:HYDR.0000041603.41913.95

Bellinger, B. J., B. A. S. Van Mooy, J. B. Cotner, and others. 2014. Physiological modifications of seston in response to physicochemical gradients within Lake Superior. Limnology & Oceanography **59**: 1011–1026. doi:10.4319/lo.2014.59.3.1011

Bottrell, H. H., A. Duncan, Z. Gliwicz, and others. 1976. Review of some problems in zooplankton production studies. Norwegian Journal of Zoology **21**: 477–483.

Bullejos, F. J., P. Carrillo, E. Gorokhova, J. M. Medina-Sánchez, E. G. Balseiro, and M. Villar-Argaiz. 2014. Shifts in food quality for herbivorous consumer growth: multiple golden means in the life history. Ecology **95**: 1272–1284. doi:10.1890/13-0410.1

Burgess, S., E. W. Jackson, L. Schwarzman, N. Gezon, and J. T. Lehman. 2015. Improved estimates of calanoid copepod biomass in the St. Lawrence Great Lakes. Journal of Great Lakes Research **41**: 484–491. doi:10.1016/j.jglr.2015.02.007

Burns, C. W. 1968. The relationship between body size of filter-feeding cladocera and the maximum size of particle ingested. Limnology and Oceanography **13**: 675–678. doi:10.4319/lo.1968.13.4.0675

Burns, C. W. 1969. Relation between filtering rate, temperature, and body size in four species of *Daphnia*. Limnology and Oceanography **14**: 693–700. doi:10.4319/lo.1969.14.5.0693

Carrillo, P., M. Villar-Argaiz, and J. M. Medina-Sánchez. 2001. Relationship between N:P ratio and growth rate during the life cycle of calanoid copepods: An in situ Measurement. Journal of Plankton Researcg **23**: 537–547. doi:10.1093/plankt/23.5.537

Carpenter, S. R., N. F. Caraco, D. L. Correll, R. W. Howarth, A. N. Sharpley, and V. H. Smith. 1998. Nonpoint pollution of surface waters with phosphorus and nitrogen. Ecological Applications **8**: 559–568. doi:10.1890/1051-0761(1998)008[0559:NPOSWW]2.0.CO;2

Checchetto, V., E. Formentin, L. Carraretto, A. Segalla, G. M. Giacometti, I. Szabo, and E. Bergantino. 2013. Functional characterization and determination of the physiological role of a calcium-dependent potassium channel from cyanobacteria. Plant Physiology **162**: 953–964. doi:10.1104/pp.113.215129

Chunyan, L., Z. Xiangchi, L. Chao, and L. Cheng. 2022. Ionomic and metabolic responses of wheat seedlings to PEG-6000-simulated drought stress under two phosphorus levels. PLOS One **17**: e0274915. doi:10.1371/journal.pone.0274915

Conley, D. J., S. S. Kilham, E. Theriot. 1989. Differences in silica content between marine and freshwater diatoms. Limnology and Oceanography **34**: 205-212. doi:10.4319/lo.1989.34.1.0205

Cowles, T. J., R. J. Olson, and S. W. Chisholm. 1988. Food selection by copepods: discrimination on the basis of food quality. Marine Biology **100**: 41–49. doi:10.1007/BF00392953

Culver, D., M. Boucherle, D. Bean, and J. Fletcher. 1985. Biomass of freshwater crustacean zooplankton from length-weight regressions. Canadian Journal of Fisheries and Aquatic Sciences **42**: 1380–1390. doi:10.1139/f85-173

Daneshgar, S., A. Callegari, A. G. Capodaglio, and D. Vaccari. 2018. The potential phosphorus crisis: Resource conservation and possible escape technologies: A Review. Resources **7**: 37. doi:10.3390/resources7020037

Davison, W. 1993. Iron and manganese in lakes. Earth-Science Reviews **34**: 119-163. doi: 10.1016/0012-8252(93)90029-7

DeMott, W. R. 1986. The role of taste in food selection by freshwater zooplankton. Oecologia **69**: 334–340. doi:10.1007/BF00377053

DeMott, W. R., R. D. Gulati, and K. Siewert. 1998. Effects of phosphorus-deficient diets on the carbon and phosphorus balance of *Daphnia magna*. Limnology and Oceanography **43**: 1147–1161. doi:10.4319/lo.1998.43.6.1147

De Senerpont Domis, L. N., D. B. Van de Waal, N. R. Helmsing, E. Van Donk, and Wolf. M. Mooij. 2014. Community stoichiometry in a changing world: combined effects of warming and eutrophication on phytoplankton dynamics. Ecology **95**: 1485–1495. doi:10.1890/13-1251.1

Dey, S., B. Tripathy, M. S. Kumar, and A. P. Das. 2023. Ecotoxicological consequences of manganese mining pollutants and their biological remediation. Environmental Chemistry and Ecotoxicology **5**: 55–61. doi:10.1016/j.enceco.2023.01.001

Diehl, S., S. Berger, R. Ptacnik, and A. Wild. 2002. Phytoplankton, light, and nutrients in a gradient of mixing depths: Field experiments. Ecology **83**: 399–411. doi:10.1890/0012-9658(2002)083[0399:PLANIA]2.0.CO;2

Dittrich, M., and M. Obst. 2004. Are picoplankton responsible for calcite precipitation in lakes? AMBIO: A Journal of the Human Environment **33**: 559–564. doi:10.1579/0044-7447-33.8.559

Downing, J. A. 1997. Marine nitrogen: Phosphorus stoichiometry and the global N:P cycle. Biogeochemistry **37**: 237–252. doi:10.1023/A:1005712322036

Dumont, H. J., I. Van de Velde, and S. Dumont. 1975. The dry weight estimate of biomass in a selection of *Cladocera*, *Copepoda* and *Rotifera* from the plankton, periphyton and benthos of continental waters. Oecologia **19**: 75–97. doi:10.1007/BF00377592

Ebert, D. 2005. Ecology, epidemiology, and evolution of parasitism in *Daphnia*. U.S. National Library of Medicine, National Center for Biotechnology Information, Bethesda, Maryland, USA.

Elser, J. J., M. M. Elser, N. A. MacKay, and S. R. Carpenter. 1988. Zooplankton-mediated transitions between N- and P-limited algal growth. Limnology and Oceanography **33**: 1–14. doi:10.4319/lo.1988.33.1.0001

Elser, J. J., D. Dobberfuhl, N. MacKay, and J. Schampel. 1996. Organism size, life history, and N:P stoichiometry. Bioscience **46**: 674–84. doi:10.2307/1312897

Elser, J. J., and J. Urabe. 1999. The stoichiometry of Consumer-Driven Nutrient Recycling: Theory, observations, and consequences. Ecology **80**: 735–751. doi:10.1890/0012-9658(1999)080[0735:TSOCDN]2.0.CO;2

Elser, J. J., and others. 2000. Biological stoichiometry from genes to ecosystems. Ecology Letters **3**: 540–550. doi:10.1111/j.1461-0248.2000.00185.x

Elser, J. J., K. Hayakawa, and J. Urabe. 2001. Nutrient limitation reduces food quality for zooplankton: *Daphnia* response to seston phosphorus enrichment. Ecology **82**: 898–903. doi:10.1890/0012-9658(2001)082[0898:NLRFQF]2.0.CO;2

Elser, J. J. and others. 2003. Growth rate–stoichiometry couplings in diverse biota. Ecology Letters **6**: 936–943. doi:10.1046/j.1461-0248.2003.00518.x

Elser, J. J. and others. 2007. Global analysis of nitrogen and phosphorus limitation of primary producers in freshwater, marine and terrestrial ecosystems. Ecology Letters **10**: 1135–1142. doi:10.1111/j.1461-0248.2007.01113.x

Ewers, L. A. 1936. Propagation and rate of reproduction of some freshwater *Copepoda*. Transactions of the American Microscopical Society **55**: 230-238. doi: 10.2307/3222616

Falkowski, P. G., and J. A. Raven. 2007. Aquatic Photosynthesis: (Second Edition), STU-Student edition. Princeton University Press.

Filstrup, C. T., and O. T. Lind. 2010. Sediment transport mechanisms influencing spatiotemporal resuspension patterns in a shallow, polymictic reservoir. Lake and Reservoir Management **26**: 85–94. doi:10.1080/07438141.2010.490771

Fox, J. and others. 2024. car: Companion to applied regression. https://cran.r-project.org/web/packages/car/index.html

Frost, P. C., M. A. Evans-White, Z. V. Finkel, T. C. Jensen, and V. Matzek. 2005. Are you what you eat? Physiological constraints on organismal stoichiometry in an elementally imbalanced world. Oikos **109**: 18–28. doi:10.1111/j.0030-1299.2005.14049.x

Frost, P. C., J. P. Benstead, W. F. Cross, H. Hillebrand, J. H. Larson, M. A. Xenopoulos, and T. Yoshida. 2006. Threshold elemental ratios of carbon and phosphorus in aquatic consumers. Ecology Letters **9**: 774–779. doi:10.1111/j.1461-0248.2006.00919.x

Geider, R. J. 1987. Light and temperature dependence of the carbon to Chlorophyll a ratio in microalgae and cyanobacteria: Implications for physiology and growth of phytoplankton. The New Phytologist **106**: 1-24. doi:10.1111/j.1469-8137.1987.tb04788.x

Geller, W., and H. Müller. 1981. The filtration apparatus of *Cladocera*: Filter mesh-sizes and their implications on food selectivity. Oecologia **49**: 316–321. doi:10.1007/BF00347591

Glass, J. B., F. Wolfe-Simon, J. J. Elser, and A. D. Anbar. 2010. Molybdenum—nitrogen co-limitation in freshwater and coastal heterocystous cyanobacteria. Limnology and Oceanography **55**: 667–676. doi:10.4319/lo.2010.55.2.0667

Greenacre, M., E. Grunsky, and J. Bacon-Shone. 2021. A comparison of isometric and amalgamation logratio balances in compositional data analysis. Computers & Geosciences **148**: 104621. doi:10.1016/j.cageo.2020.104621

Gurney, W. S. C., E. Mccauley, R. M. Nisbet, and W. W. Murdoch. The physiological ecology of *Daphnia*: A dynamic model of growth and reproduction. Ecology **71**: 716-732. doi: 0.2307/1940325

Håkanson, L. 2005. The importance of lake morphometry for the structure and function of lakes. International Review of Hydrobiology **90**: 433–461. doi:10.1002/iroh.200410775

Hamilton-Taylor, J., and W. Davison. 1995. Redox-driven cycling of trace elements in lakes. In: Lerman, A., Imboden, D.M., Gat, J.R. (eds) Physics and Chemistry of Lakes. Springer. doi: 10.1007/978-3-642-85132-2_8

Hampton, S. E., M. V. Moore, T. Ozersky, E. H. Stanley, C. M. Polashenski, and A. W. E. Galloway. 2015. Heating up a cold subject: prospects for under-ice plankton research in lakes. Journal of Plankton Research **37**: 277–284. doi:10.1093/plankt/fbv002

Haney, J. F., and D. J. Hall. 1973. Sugar-coated *Daphnia*: A preservation technique for Cladocera. Limnology and Oceanography **18**: 331–333. doi:10.4319/lo.1973.18.2.0331

He, X., and W. X. Wang. 2008. Stoichiometric regulation of carbon and phosphorus in P-deficient *Daphnia magna*. Limnology & Oceanography **53**: 244–254. doi:10.4319/lo.2008.53.1.0244

Hecky, R. E., and P. Kilham. 1988. Nutrient limitation of phytoplankton in freshwater and marine environments: A review of recent evidence on the effects of enrichment. Limnology and Oceanography **33**: 796–822. doi:10.4319/lo.1988.33.4part2.0796

Herstoff, E. M., C. L. Meunier, M. Boersma, and S. Baines. 2023. Are all copepods the same? Variation in copepod stoichiometry with taxonomy, ontogeny, latitude, and habitat. Ecosphere **14**: e4705. doi:10.1002/ecs2.4705

Hessen, D. O., and Lyche, A. 1991. Inter- and intraspecific variations in zooplankton element composition. Archiv für Hydrobiologie **121**: 343-353.

Hessen, D. O., E. van Donk, and R. Gulati. 2005. Seasonal seston stoichiometry: effects on zooplankton in cyanobacteria-dominated lakes. Journal of Plankton Research **27**: 449–460. doi:10.1093/plankt/fbi018

Hessen, D. O., and T. R. Anderson. 2008. Excess carbon in aquatic organisms and ecosystems: Physiological, ecological, and evolutionary implications. Limnology and Oceanography **53**: 1685–1696. doi:10.4319/lo.2008.53.4.1685

Hessen, D. O., J. J. Elser, R. W. Sterner, and J. Urabe. 2013. Ecological stoichiometry: An elementary approach using basic principles. Limnology and Oceanography **58**: 2219–2236. doi:10.4319/lo.2013.58.6.2219

Hessen, D. O., O. T. Hafslund, T. Andersen, C. Broch, N. K. Shala, and M. W. Wojewodzic. 2017. Changes in stoichiometry, cellular RNA, and alkaline phosphatase activity of Chlamydomonas in response to temperature and nutrients. Frontiers in Microbiology **8**. doi:10.3389/fmicb.2017.00018

Hilton, J. 1985. A conceptual framework for predicting the occurrence of sediment focusing and sediment redistribution in small lakes. Limnology and Oceanography **30**: 1131–1143. doi:10.4319/lo.1985.30.6.1131

Hirst, A., and A. McKinnon. 2001. Does egg production represent adult female copepod growth? A call to account for body weight changes. Marine Ecology Progress Series **223**: 179–199. doi:10.3354/meps223179

Ho, T., A. Quigg, Z. V. Finkel, A. J. Milligan, K. Wyman, P. G. Falkowski, and F. M. M. Morel. 2003. The elemental composition of some marine phytoplankton. Journal of Phycology **39**: 1145–1159. doi:10.1111/j.0022-3646.2003.03-090.x

Hodell, D. A., C. L. Schelske, G. L. Fahnenstiel, and L. L. Robbins. 1998. Biologically induced calcite and its isotopic composition in Lake Ontario. Limnology and Oceanography **43**: 187–199. doi:10.4319/lo.1998.43.2.0187

Jensen, K. H., P. Larsson, and G. Högstedt. 2001. Detecting food search in *Daphnia* in the field. Limnology and Oceanography **46**: 1013–1020. doi:10.4319/lo.2001.46.5.1013

Jeyasingh, P. D., J. M. Goos, S. K. Thompson, C. M. Godwin, and J. B. Cotner. 2017. Ecological stoichiometry beyond Redfield: An ionomic perspective on elemental homeostasis. Frontiers in Microbiology **8**: 722. https://doi.org/10.3389/fmicb.2017.00722

Jeyasingh, P. D., J. M. Goos, P. R. Lind, P. Roy Chowdhury, and R. E. Sherman. 2020. Phosphorus supply shifts the quotas of multiple elements in algae and *Daphnia*: ionomic basis of stoichiometric constraints. Ecology Letters **23**: 1064–1072. doi:10.1111/ele.13505

Jeyasingh, P. D., R. E. Sherman, C. Prater, K. Pulkkinen, and T. Ketola. 2023. Adaptation to a limiting element involves mitigation of multiple elemental imbalances. Journal of the Royal Society Interface. **20**: 20220472. doi:10.1098/rsif.2022.0472

Khattak, H. K., C. Prater, N. D. Wagner, and P. C. Frost. 2018. The threshold elemental ratio of carbon and phosphorus of *Daphnia magna* and its connection to animal growth. Scientific Reports **8**: 9673. doi:10.1038/s41598-018-27758-7

Kelly, P. T., J. M. Taylor, I. M. Andersen, and J. T. Scott. 2024. Zooplankton densities reduced by increases in resource N:P in hypereutrophic mesocosms. Hydrobiologia. doi:10.1007/s10750-024-05557-8

Korkmaz, S., D. Goksuluk, and G. Zararsiz. 2025. MVN: Multivariate Normality Tests. https://cran.r-project.org/web/packages/MVN/index.html

Lampert, W. 1987. Laboratory studies on zooplankton-cyanobacteria interactions. New Zealand Journal of Marine and Freshwater Research **21**: 483–490. doi:10.1080/00288330.1987.9516244

Laws, E. A., and T. T. Bannister. 1980. Nutrient- and light-limited growth of *Thalassiosira fluviatilis* in continuous culture, with implications for phytoplankton growth in the ocean. Limnology & Oceanography **25**: 457–473. doi:10.4319/lo.1980.25.3.0457

Leibold, M. A. 1990. Resources and predators can affect the vertical distributions of zooplankton. Limnology and Oceanography **35**: 938–944. doi:10.4319/lo.1990.35.4.0938

Lüdecke, D., Ben-Shachar, M.S., Patil, I., Waggoner, P., Makowski, D. 2021. performance: An R package for assessment, comparison and testing of statistical

models. Journal of Open Source Software, 6(60), 3139. https://doi.org/10.21105/joss.03139
Mackereth, F. J. H. 1997. Chemical investigation of lake sediments and their interpretation. Proceedings of the Royal Society of London. Series B. Biological Sciences **161**: 295–309. doi:10.1098/rspb.1965.0002
Malzahn, A. M., D. Doerfler, and M. Boersma. 2016. Junk food gets healthier when it's warm. Limnology and Oceanography **61**: 1677–1685. doi:10.1002/lno.10330
Mathews, L., C. L. Faithfull, P. H. Lenz, and C. E. Nelson. 2018. The effects of food stoichiometry and temperature on copepods are mediated by ontogeny. Oecologia **188**: 75–84. doi:10.1007/s00442-018-4183-6
McCarthy, S. D. S., S. P. Rafferty, and P. C. Frost. 2010. Responses of alkaline phosphatase activity to phosphorus stress in *Daphnia magna*. Journal of Experimental Biology **213**: 256–261. doi:10.1242/jeb.037788
McCauley, E., W. W. Murdoch, R. M. Nisbet, and W. S. C. Gurney. 1990. The physiological ecology of *Daphnia*: Development of a model of growth and reproduction. Ecology **71**: 703-715. doi: 10.2307/1940324
McFeeters, B. J., and P. C. Frost. 2011. Temperature and the effects of elemental food quality on *Daphnia*. Freshwater Biology **56**: 1447–1455. doi:10.1111/j.1365-2427.2011.02586.x
Meunier, C. L., M. Boersma, K. H. Wiltshire, and A. M. Malzahn. 2016. Zooplankton eat what they need: copepod selective feeding and potential consequences for marine systems. Oikos 125: 50–58. doi:10.1111/oik.02072
Misson, J., K. G. Raghothama, A. Jain, and others. 2005. A genome-wide transcriptional analysis using *Arabidopsis thaliana* Affymetrix gene chips determined plant responses to phosphate deprivation. Proceedings of the National Academy of Sciences **102**: 11934–11939. doi:10.1073/pnas.0505266102
Moody, E. K., A. T. Rugenski, J. L. Sabo, B. L. Turner, and J. J. Elser. 2017. Does the growth rate hypothesis apply across temperatures? Variation in the growth rate and body phosphorus of neotropical benthic grazers. Frontiers in Environmental Science **5**. doi:10.3389/fenvs.2017.00014
Nguyen, N.-L., V.-H. Bui, H.-N. Pham, H.-M. To, M.-G. Dijoux-Franca, C.-T. Vu, and K.-O. T. Nguyen. 2022. Ionomics and metabolomics analysis reveal the molecular mechanism of metal tolerance of *Pteris vittata L*. dominating in a mining site in Thai Nguyen province, Vietnam. Environmental Science and Pollution Research **29**: 87268–87280. doi:10.1007/s11356-022-21820-8
Ochoa-Hueso, R. and others. 2023. Bioavailability of macro and micronutrients across global topsoils: Main drivers and global change impacts. Global Biogeochemical Cycles **37**: e2022GB007680. doi:10.1029/2022GB007680
Otsuki, A., and R. G. Wetzel. 1972. Coprecipitation of phosphate with carbonates in a marl lake. Limnology and Oceanography **17**: 763–767. doi:10.4319/lo.1972.17.5.0763
Paerl, H. W., J. T. Scott, M. J. McCarthy, and others. 2016. It takes two to tango: When and where dual nutrient (N & P) reductions are needed to protect lakes and

downstream ecosystems. Environmental Science and Technology **50**: 10805–10813. doi:10.1021/acs.est.6b02575

Parent, S.-É., L. E. Parent, J. J. Egozcue, and others. 2013. The plant ionome revisited by the nutrient balance concept. Frontiers in Plant Science **4**. doi:10.3389/fpls.2013.00039

Persson, J., and T. Vrede. 2006. Polyunsaturated fatty acids in zooplankton: variation due to taxonomy and trophic position. Freshwater Biology **51**: 887-900. doi: 10.1111/j.1365-2427.2006.01540.x

Persson, J., P. Fink, A. Goto, J. M. Hood, J. Jonas, and S. Kato. 2010. To be or not to be what you eat: regulation of stoichiometric homeostasis among autotrophs and heterotrophs. Oikos **119**: 741–751. doi:10.1111/j.1600-0706.2009.18545.x

Pohland, A.-C., and D. Schneider. 2019. Mg^{2+} homeostasis and transport in cyanobacteria – at the crossroads of bacterial and chloroplast Mg^{2+} import. Biological Chemistry **400**: 1289–1301. doi:10.1515/hsz-2018-0476

Prater, C., N. D. Wagner, and P. C. Frost. 2018. Seasonal effects of food quality and temperature on body stoichiometry, biochemistry, and biomass production in *Daphnia* populations. Limnology and Oceanography **63**: 1727–1740. doi:10.1002/lno.10803

Quigg, A. and others. 2003. The evolutionary inheritance of elemental stoichiometry in marine phytoplankton. Nature **425**: 291–294. doi:10.1038/nature01953

R Core Team. 2023. R: A language and environment for statistical computing. R Foundation for Statistical Computing, Vienna, Austria. https://www.R-project.org/

Ragueneau, O. and others. 2000. A review of the Si cycle in the modern ocean: recent progress and missing gaps in the application of biogenic opal as a paleoproductivity proxy. Global and Planetary Change **26**: 317–365. doi:10.1016/S0921-8181(00)00052-7

Raven, J. A. 2012. Protein turnover and plant RNA and phosphorus requirements in relation to nitrogen fixation. Plant Science **188–189**: 25–35. doi:10.1016/j.plantsci.2012.02.010

Reynolds, C. S. 1984. The ecology of freshwater phytoplankton, Cambridge University Press.

Reynolds, B. C. 2009. Modeling the modern marine δ30Si distribution. Global Biogeochemical Cycles **23**. doi:10.1029/2008GB003266

Rosen, R.A. 1981. Length-dry weight relationships of some freshwater zooplankton. Journal of Freshwater Ecology 1:225-229. doi: 10.1080/02705060.1981.9664034

Rühland, K., A. M. Paterson, and J. P. Smol. 2008. Hemispheric-scale patterns of climate-related shifts in planktonic diatoms from North American and European lakes. Global Change Biology **14**: 2740–2754. doi:10.1111/j.1365-2486.2008.01670.x

Salt, D. E., I. Baxter, and B. Lahner. 2008. Ionomics and the study of the plant ionome. Annual Review of Plant Biology **59**: 709–733. doi:10.1146/annurev.arplant.59.032607.092942

Schindler, D. W., P. J. Curtis, B. R. Parker, and M. P. Stainton. 1996. Consequences of climate warming and lake acidification for UV-B penetration in North American boreal lakes. Nature **379**: 705–708. doi:10.1038/379705a0

Schindler, D. W. 2012. The dilemma of controlling cultural eutrophication of lakes. Proceedings of the Royal Society B: Biological Sciences **279**: 4322–4333. doi:10.1098/rspb.2012.1032

Schindler, D. W., S. R. Carpenter, S. C. Chapra, R. E. Hecky, and D. M. Orihel. 2016. Reducing phosphorus to curb lake eutrophication is a success. Environmental Science & Technology. **50**: 8923–8929. doi:10.1021/acs.est.6b02204

Schneider, B., and M. Kabeláč. 1998. Stereochemistry of binding of metal cations and water to a phosphate group. Journal of the American Chemical Society **120**: 161–165. doi:10.1021/ja972237+

Scholtysik, G., T. Goldhammer, H. W. Arz, M. Moros, R. Littke, and M. Hupfer. 2022. Geochemical focusing and burial of sedimentary iron, manganese, and phosphorus during lake eutrophication. Limnology and Oceanography **67**: 768–783. doi:10.1002/lno.12019

Sen, I. S., and B. Peucker-Ehrenbrink. 2012. Anthropogenic disturbance of element cycles at the Earth's surface. Environmental Science & Technology **46**: 8601–8609. doi:10.1021/es301261x

Silva, A. R. da. 2025. biotools: Tools for Biometry and Applied Statistics in Agricultural Science. https://cran.r-project.org/web/packages/biotools/index.html

Smol, J. P. 1988. Paleoclimate proxy data from freshwater arctic diatoms. Internationale Vereinigung für theoretische und angewandte Limnologie: Verhandlungen 23: 837-844. doi: 10.1080/03680770.1987.11899722

Somero, G. N. 2004. Adaptation of enzymes to temperature: searching for basic "strategies." Comparative Biochemistry and Physiology Part B: Biochemistry and Molecular Biology **139**: 321–333. doi:10.1016/j.cbpc.2004.05.003

Sommer, U., Z. M. Gliwicz, W. Lampert, and A. Duncan. 1986. The PEG-model of seasonal succession of planktonic events in fresh waters. Archiv Hydrobiologie **106**: 433–471. doi:10.1127/archiv-hydrobiol/106/1986/433

Sommer, U., and F. Sommer. 2006. Cladocerans versus copepods: the cause of contrasting top–down controls on freshwater and marine phytoplankton. Oecologia **147**: 183–194. doi:10.1007/s00442-005-0320-0

Søndergaard, M., J. P. Jensen, and E. Jeppesen. 2003. Role of sediment and internal loading of phosphorus in shallow lakes. Hydrobiologia **506**: 135–145. doi:10.1023/B:HYDR.0000008611.12704.dd

Stabel, H.-H. 1986. Calcite precipitation in Lake Constance: Chemical equilibrium, sedimentation, and nucleation by algae. Limnology and Oceanography **31**: 1081–1094. doi:10.4319/lo.1986.31.5.1081

Sterner, R. W. 1989. Resource competition during seasonal succession toward dominance by cyanobacteria. Ecology **70**: 229–245. doi:10.2307/1938429

Sterner, R. W., D. D. Hagemeier, W. L. Smith, and R. F. Smith. 1993. Phytoplankton nutrient limitation and food quality for *Daphnia*. Limnology and Oceanography **38**: 857–871. doi:10.4319/lo.1993.38.4.0857

Sterner, R. W., and M. S. Schwalbach. 2001. Diel integration of food quality by *Daphnia*: Luxury consumption by a freshwater planktonic herbivore. Limnology and Oceanography **46**: 410–416. doi:10.4319/lo.2001.46.2.0410

Sterner, R. W., Elser, J. J. 2002. Ecological Stoichiometry: The biology of elements from molecules to the biosphere. Princeton University Press, Princeton.

Stroud Water Research Center. 2017. Model my watershed [Software]. Available from https://wikiwatershed.org/

Stumm, W. and Morgan, J.J. (1996) Aquatic chemistry, chemical equilibria and rates in natural waters. 3rd Edition, John Wiley & Sons, Inc., New York. Scientific Research Publishing.

Tchounwou, P. B., C. G. Yedjou, A. K. Patlolla, and D. J. Sutton. 2012. Heavy metal toxicity and the environment, p. 133–164. *In* A. Luch [ed.], Molecular, Clinical and Environmental Toxicology: Volume 3: Environmental Toxicology. Springer.

Tiselius, P., and P. Jonsson. 1990. Foraging behaviour of six calanoid copepods: observations and hydrodynamic analysis. Marine Ecology Progress Series **66**: 23–33. doi:10.3354/meps066023

Urabe, J., and Y. Watanabe. 1992. Possibility of N or P limitation for planktonic cladocerans: An experimental test. Limnology and Oceanography **37**: 244–251. doi:10.4319/lo.1992.37.2.0244

Urabe, J. 1995. Direct and indirect effects of zooplankton on seston stoichiometry. Écoscience **2**, 286-296. doi: 10.1080/11956860.1995.11682296

Urabe, J., J. Togari, and J. J. Elser. 2003. Stoichiometric impacts of increased carbon dioxide on a planktonic herbivore. Global Change Biology **9**: 818–825. doi:10.1046/j.1365-2486.2003.00634.x

van den Boogaart, K. G., and R. Tolosana-Delgado. 2008. "compositions": A unified R package to analyze compositional data. Computers & Geosciences **34**: 320–338. doi:10.1016/j.cageo.2006.11.017

Van Mooy, B. A. S., H. F. Fredricks, B. E. Pedler, and others. 2009. Phytoplankton in the ocean use non-phosphorus lipids in response to phosphorus scarcity. Nature **458**: 69–72. doi:10.1038/nature07659

Villar-Argaiz, M., J. M. Medina-Sánchez, and P. Carrillo. 2002. Linking life history strategies and ontogeny in crustacean zooplankton: Implications for homeostasis. Ecology **83**: 1899–1914. doi:10.1890/0012-9658(2002)083[1899:LLHSAO]2.0.CO;2

Vitousek, P. M., J. D. Aber, R. W. Howarth, G. E. Likens, P. A. Matson, D. W. Schindler, W. H. Schlesinger, and D. G. Tilman. 1997. Human alteration of the global nitrogen cycle: Sources and consequences. Ecological Applications **7**: 737–750. doi:10.1890/1051-0761(1997)007[0737:HAOTGN]2.0.CO;2

Wagner, N. D., and P. C. Frost. 2012. Responses of alkaline phosphatase activity in *Daphnia* to poor nutrition. Oecologia **170**: 1–10. doi:10.1007/s00442-012-2277-0

Wagner, N. D., H. Hillebrand, A. Wacker, and P. C. Frost. 2013. Nutritional indicators and their uses in ecology. Ecology Letters **16**: 535–544. doi:10.1111/ele.12067

Wagner, N. D., B. P. Lankadurai, M. J. Simpson, A. J. Simpson, and P. C. Frost. 2015. Metabolomic differentiation of nutritional stress in an aquatic invertebrate. Physiological and Biochemical Zoology **88**: 43–52. doi:10.1086/679637

Wagner, N. D., C. Prater, and P. C. Frost. 2017. Dynamic responses of phosphorus metabolism to acute and chronic dietary phosphorus-limitation in *Daphnia*. Frontiers in Environmental Science **5**. doi:10.3389/fenvs.2017.00036

Wagner, N. D., C. Prater, C. J. Robbins, F. S. Osburn, J. Wang, P. D. Jeyasingh, and J. T. Scott. 2025. Current and historical resource nitrogen supply affects the eco-physiological traits and the ionome of a diazotrophic cyanobacterium. Ecology Letters **28**: e70051. doi:10.1111/ele.70051

Warner, K. A., R. A. Fowler, R. M. Northington, H. I. Malik, J. McCue, and J. E. Saros. 2018. How does changing ice-out affect arctic versus boreal lakes? A comparison using two years with ice-out that differed by more than three weeks. Water **10**: 78. doi:10.3390/w10010078

Watanabe, T., M. Urayama, T. Shinano, R. Okada, and M. Osaki. 2015. Application of ionomics to plant and soil in fields under long-term fertilizer trials. SpringerPlus **4**: 781. doi:10.1186/s40064-015-1562-x

Watkins, J., Rudstam, L., Holeck, K. 2011. Length-weight regressions for zooplankton biomass calculations – A review and a suggestion for standard equations. Cornell Biological Field Station Publications and Reports. https://ecommons.cornell.edu/items/5f491e81-2f43-4347-b944-ae116b41834f

Watson, S. B., E. McCauley, and J. A. Downing. 1997. Patterns in phytoplankton taxonomic composition across temperate lakes of differing nutrient status. Limnology and Oceanography **42**: 487–495. doi:10.4319/lo.1997.42.3.0487

Wang, X., T. J. Browning, E. P. Achterberg, and M. Gledhill. 2022. Phosphorus limitation enhances diazotroph zinc quotas. Frontiers in Microbiology **13**: 853519. doi:10.3389/fmicb.2022.853519

Winder, M., and U. Sommer. 2012. Phytoplankton response to a changing climate. Hydrobiologia **698**: 5–16. doi:10.1007/s10750-012-1149-2

Wetzel, R.G., 2001. Limnology: Lake and river ecosystems. Academic Press, San Diego.

Wojewodzic, M. W., M. Kyle, J. J. Elser, D. O. Hessen, and T. Andersen. 2011a. Joint effect of phosphorus limitation and temperature on alkaline phosphatase activity and somatic growth in *Daphnia magna*. Oecologia **165**: 837–846. doi:10.1007/s00442-010-1863-2

Wojewodzic, M. W., T. Rachamim, T. Andersen, H. P. Leinaas, and D. O. Hessen. 2011b. Effect of temperature and dietary elemental composition on RNA/protein ratio in a rotifer. Functional Ecology **25**: 1154–1160. doi:10.1111/j.1365-2435.2011.01864.x

Wong, M. Y., S. D. Rathod, R. Marino, and others. 2021. Anthropogenic perturbations to the atmospheric molybdenum cycle. Global Biogeochemical Cycles **35**: e2020GB006787. doi:10.1029/2020GB006787

Wurtsbaugh, W. A., H. W. Paerl, and W. K. Dodds. 2019. Nutrients, eutrophication and harmful algal blooms along the freshwater to marine continuum. WIREs Water **6**: e1373. doi:10.1002/wat2.1373

Yvon-Durocher, G., M. Dossena, M. Trimmer, G. Woodward, and A. P. Allen. 2015. Temperature and the biogeography of algal stoichiometry. Global Ecology and Biogeography **24**: 562-570. doi:10.1111/geb.12280